UNIVERSIDAD DE CONCEPCIÓN

FACULTAD DE CIENCIAS NATURALES Y OCEANOGRÁFICAS

Programa de Magíster en Ciencias con Mención en Zoología

Climatic seasonality drives clutch size macroevolution in passerine birds

Tesis presentada a la Facultad de Ciencias Naturales y Oceanográficas de
la Universidad de Concepción para optar al grado académico de
Magíster en Ciencias con mención en Zoología

Por: Joaquín José Cárcamo Gallardo

Profesor Guía: Dr. Enrique Rodríguez

Profesor Co-Guía: Dr. Cristián E. Hernández U.

Profesor Co-Guía: PhD Andrew Meade

agosto, 2026

Concepción - Chile

ORCID del autor: 0009-0005-1936-2356

ORCID del profesor guía: 0000-0002-5049-8500

AGRADECIMIENTOS

Quiero agradecer a todas las personas que me acompañaron durante este magíster y que, de distintas maneras, hicieron posible esta tesis.

En especial, agradezco a mi familia: mi mamá, Ximena; mi tía Margot; y mis primas. A pesar de la distancia, han estado presentes en cada decisión y dificultad, brindándome siempre su apoyo y confianza. A mi compañera de vida, Paula Roa, por acompañarme desde el primer año del magíster, por su paciencia y apoyo cotidiano, y por hacer mucho más llevadero este proceso. Y a Bucksita, mi perrita, que se sumó en el camino a brindar apoyo moral.

También agradezco a mis amigos de La Ballena y del Centro EULA, así como a mis colegas, amigos y profesores del Laboratorio de Dinámica Eco-Evolutiva y Filogenética de la Universidad San Sebastián y del Laboratorio de Mastozoología de la Universidad de Concepción.

Finalmente, agradezco a mi profesor guía, Dr. Enrique Rodríguez, y a mis co-guías, Dr. Cristián E. Hernández U. y Dr. Andrew Meade, por su orientación y apoyo. También agradezco al Dr. Jorge Avaria-Llautureo y al Dr. Chris Venditti, quienes, junto con Andrew, compartieron generosamente su experiencia en macroevolución, respondieron con paciencia a mis numerosas inquietudes y dedicaron su tiempo a fortalecer este trabajo.

ACKNOWLEDGMENTS

I would like to thank everyone who accompanied me throughout this master's degree and who, in different ways, made this thesis possible.

I am especially grateful to my family: my mother, Ximena; my aunt Margot; and my cousins. Despite the distance, they have supported me through every decision and difficulty, always offering their encouragement and trust. To my life partner, Paula Roa, for being beside me since the first year of my master's degree, for her patience and daily support, and for making this process much more manageable. And to Bucksita, my dog, who joined us along the way to provide moral support.

I also thank my friends from FCNO and the EULA Center at UdeC, as well as my colleagues, friends and professors from the Laboratory of Eco-Evolutionary Dynamics and Phylogenetics at Universidad San Sebastián and the Mammalogy Laboratory at Universidad de Concepción.

Finally, I thank my supervisor, Dr Enrique Rodríguez, and my co-supervisors, Dr Cristián E. Hernández U. and Dr Andrew Meade, for their guidance and support. I also thank Dr Jorge Avaria-Llautureo and Dr Chris Venditti, who, together with Andrew, generously shared their expertise in macroevolution, patiently addressed my many questions and dedicated their time to strengthening this work.

TABLE OF CONTENTS

LIST OF TABLES

LIST OF FIGURES

RESUMEN

El aumento del tamaño de nidada de las aves desde los trópicos hacia los polos se ha explicado tradicionalmente mediante la hipótesis de Ashmole, según la cual los cuellos de botella estacionales en los recursos reducen la densidad poblacional y aumentan los recursos per cápita cuando mejoran las condiciones, lo que favorece nidadas más grandes. Este mecanismo influye directamente en la adecuación biológica de las especies, por lo que su rol podría derivarse de procesos evolutivos profundos, coherentes con mecanismos poblacionales a escala ecológica. Mediante métodos filogenéticos recientemente desarrollados y un conjunto de datos de 1.663 especies de Passeriformes, evaluamos cómo este mecanismo a escala poblacional se ha traducido en diferencias macroevolutivas persistentes entre especies. Entre los factores ambientales y de historia de vida incluidos, el clima presentó la mayor contribución a la variación interespecífica en el tamaño de nidada, impulsada principalmente por la disponibilidad mínima de recursos, y se asoció con el 33,7 % de los cambios direccionales y el 21,5 % de los cambios de evolabilidad (cambios en la tasa evolutiva). El patrón latitudinal parece haber surgido de magnitudes equivalentes de cambio direccional asociado al clima que actuaron en sentidos opuestos: reducciones del tamaño medio de nidada en los linajes tropicales y aumentos en latitudes más altas. La masa corporal y la masa del huevo influyeron en el tamaño de la nidada, pero sus efectos sobre la respuesta y la historia evolutiva asociada al clima fueron, en

general, débiles y restringidos a clados particulares**.** La migración, en cambio, reveló rutas evolutivas distintas hacia respuestas contemporáneas similares: migrantes y residentes mostraron relaciones comparables entre clima y tamaño de nidada, pero los linajes residentes acumularon aumentos direccionales en el tamaño de su nidada asociados a una mayor estacionalidad climática, de acuerdo con una mayor exposición a cuellos de botella estacionales locales, mientras que la migración permite a las especies seguir los recursos estacionales e impone un conjunto distinto de presiones demográficas.

Palabras clave: tamaño de nidada; Passeriformes; hipótesis de Ashmole; estacionalidad climática; métodos comparativos filogenéticos; evolvabilidad

ABSTRACT

The increase in clutch size in birds from the tropics to the poles has traditionally been explained by the Ashmole hypothesis, which holds that seasonal resource bottlenecks reduce population density and increase per capita resources when conditions improve, favouring larger clutches. This mechanism directly influences species fitness, so its role may reflect deep evolutionary processes consistent with population mechanisms at the ecological scale. Using newly developed phylogenetic methods and a dataset of 1,663 Passeriformes species, we assessed how this population-scale mechanism has translated into persistent macroevolutionary differences between species. Among the environmental and life-history factors included, climate made the largest contribution to interspecific variation in clutch size, driven mainly by minimum resource availability, and was associated with 33.7% of directional changes and 21.5% of evolvability changes (changes in evolutionary rate). The latitudinal pattern appears to have arisen from equivalent magnitudes of climate-related directional change acting in opposite directions: reductions in average clutch size in tropical lineages and increases at higher latitudes. Body mass and egg mass influenced clutch size, but their effects on climatic responses and climate-associated evolutionary history were generally weak and restricted to particular clades.

Migration, on the other hand, revealed distinct evolutionary pathways toward similar contemporaneous responses: migrants and residents showed comparable relationships between climate and clutch size, but resident lineages accumulated

positive directional changes associated with stronger climatic seasonality due to greater exposure to local seasonal bottlenecks, while migration allows species to follow seasonal resources and imposes a distinct set of demographic pressures.

Keywords: clutch size; Passeriformes; Ashmole's hypothesis; climatic seasonality; phylogenetic comparative methods; evolvability

INTRODUCTION

Clutch size is a major component of avian reproductive fitness (Rowe et al., 1994; Stearns, 1992). Under David Lack's optimality theory, natural selection favours clutch sizes that maximise the number of offspring parents can successfully rear (Lack, 1947). Local environmental conditions can shift this reproductive optimum, generating variation in clutch size among individuals, populations and species, and even within the same female across breeding attempts as climatic conditions change (Chik et al., 2022; Hidalgo Aranzamendi et al., 2019; Martin et al., 2025). Understanding the evolutionary origin of this variation has therefore been a longstanding question in evolutionary ecology (Pincheira-Donoso & Hunt, 2017). Despite variation arising across multiple biological levels, clutch size shows a broad geographical pattern: mean clutch size increases from the tropics toward the poles. Since this pattern was first documented in the 1940s (Lack, 1947; Moreau, 1944), numerous explanations have been proposed, invoking geographical variation in food availability, day length, predation and adult mortality (Ricklefs, 2000).

Ashmole's hypothesis provides a unifying demographic mechanism for clutch size variation by linking seasonal resource limitation, population density, and reproductive investment. Under this framework, resource limitation during the least productive part of the annual cycle reduces population density through density-dependent mortality. When resources subsequently increase, the

surviving population experiences greater per-capita resource availability, allowing greater reproductive investment and larger clutches (Ashmole, 1961; Ashmole, 1963; Lundblad & Conway, 2021). This mechanism generates three principal related predictions: (I) clutch size should increase with the seasonal contrast in resource availability, being larger where maximum resources are high relative to minimum resources; (II) clutch size should decrease with minimum resource availability; and (III) variation in minimum resource availability should be more strongly associated with clutch size than variation in maximum resource availability.

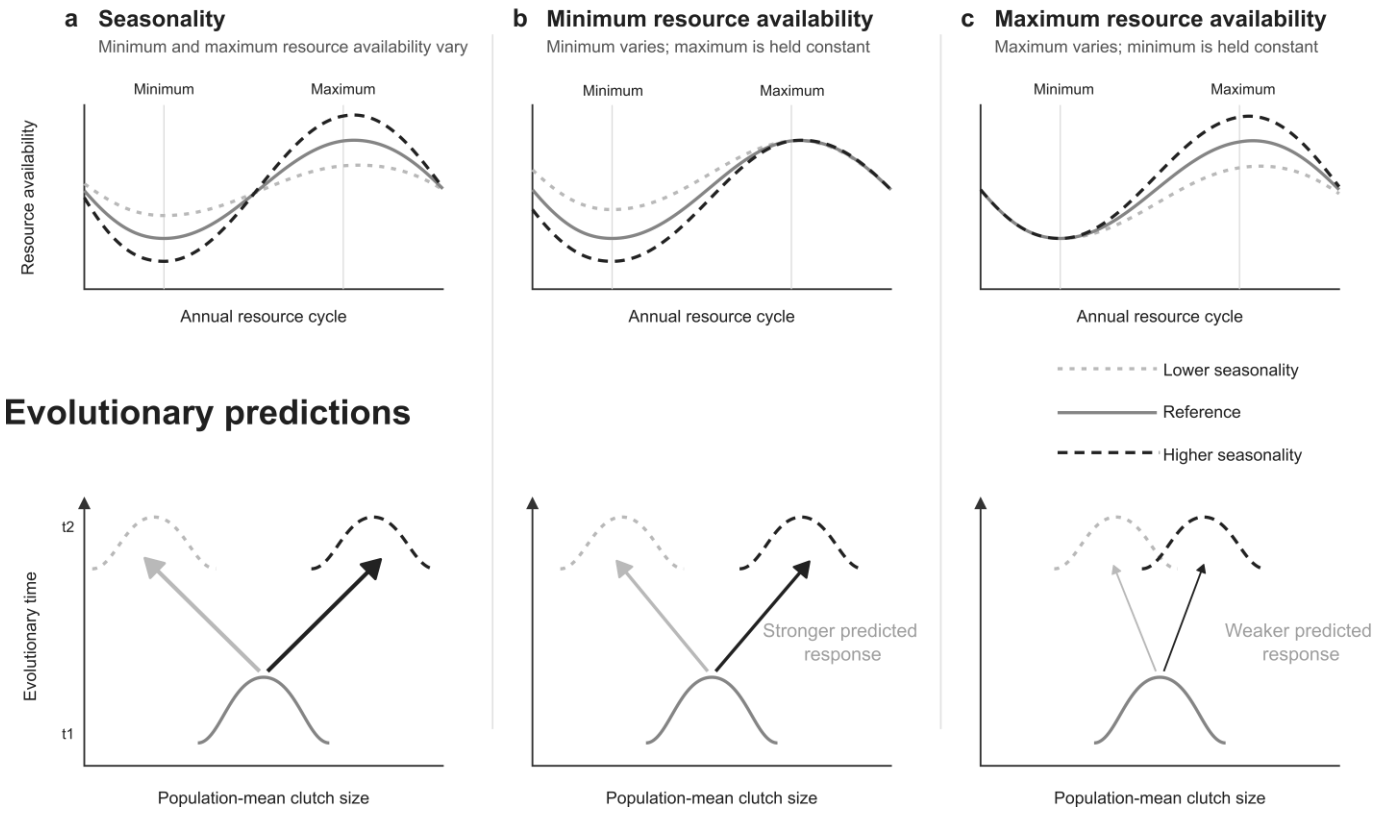

Figure 1. Conceptual predictions of Ashmole's hypothesis. a, Resource seasonality varies through joint changes in minimum and maximum resource availability; greater seasonal contrast is predicted to favour larger population-mean clutch sizes (prediction I). **b,** increasing minimum resource availability while maximum availability remains constant is predicted to reduce clutch size (prediction II). **c,** Changes in maximum resource availability are predicted to have a weaker effect than equivalent changes in minimum availability; thus, the response in **b** is expected to

exceed that in **c** (prediction III). Light dotted, solid grey and black dashed curves represent lower, reference and higher resource availability or seasonality, respectively.

Evidence consistent with Ashmole's first prediction has been documented in both endothermic and ectothermic vertebrates, with measures of environmental or resource seasonality often explaining fecundity patterns better than absolute, mean or maximum resource availability (Griebeler et al., 2010; Hořák et al., 2015; Jetz et al., 2008; Lundblad & Conway, 2021, 2023; Meiri et al., 2020; Tökölyi et al., 2014; Youngflesh et al., 2025). However, most tests have focused on the general effect of seasonality, frequently approximating resources indirectly through temperature, whereas direct evaluations of the second and third predictions remain comparatively scarce (Lundblad & Conway, 2021). More fundamentally, Ashmole's hypothesis describes an ecological and demographic mechanism operating within populations, yet it is invoked to explain an emergent pattern among species (Pincheira-Donoso & Hunt, 2017). Although clutch size is highly plastic (Haywood, 2013), quantitative-genetic studies in intensively monitored wild passerine populations have repeatedly detected additive genetic variance in the trait, with narrow-sense heritability estimates of approximately $h^2 = 0.24$ in independent populations of *Parus major (Evans et al., 2020; Ramakers et al., 2018)*, alongside evidence from other passerine systems (Husby et al., 2015; Postma & van Noordwijk, 2005). Recurrent selection under contrasting regimes of seasonal resource limitation could therefore translate population-level ecological responses into persistent differences in clutch size among species,

consistent with global comparative evidence linking avian clutch size to environmental seasonality (Jetz et al., 2008). Accumulated over evolutionary time, such responses could also contribute to lineage-specific changes in the direction or tempo of clutch-size evolution. Ashmole's demographic mechanism thus provides a plausible pathway through which ecological seasonality could generate macroevolutionary divergence.

Under the simplest macroevolutionary scenario, present-day variation in clutch size could emerge through a homogeneous Brownian-motion process, in which all lineages share a common evolutionary rate and phenotypic changes are directionally unbiased (Felsenstein, 1985; Revell et al., 2008). Under this expectation, trait variance increases with phylogenetic time, but there is no persistent tendency towards larger or smaller trait values (O'Meara et al., 2006). Evolutionary change, however, can depart from this homogeneous process in both its rate and direction (Gould, 1988). Rates of phenotypic evolution may vary among lineages and through time, concentrating change in particular branches or periods (Uyeda et al., 2011), while directional shifts can bias evolutionary trajectories towards higher or lower trait values (Pagel et al., 2022). For clutch size, recurrent differences in seasonal resource limitation provide an explicit ecological mechanism that could generate both forms of heterogeneity, altering not only how much evolutionary change accumulates across lineages, but also the direction in which clutch size evolves.

Although seasonal resource availability provides the ecological context for evolving smaller or larger clutches, species' capacity to translate resource pulses into reproductive output depends on intrinsic life-history constraints (Griebeler & Böhning-Gaese, 2004). The metabolic theory of ecology provides a common framework for these constraints, linking body size to reproductive rates through size-dependent metabolism (Brown et al., 2004; Brown et al., 2018; Brown & Sibly, 2006; Burger et al., 2019; Sibly, Kodric-Brown, et al., 2012; Sibly, Witt, et al., 2012). Calder's rule predicts declining clutch size with increasing body size (Boyer et al., 2010; Calder, 1984), consistent with lower mass-specific production in larger species (Burger et al., 2019; Okie et al., 2013), although the strength and direction of this relationship vary across avian lineages and taxonomic scales, with positive associations occurring within some clades (Boyer et al., 2010; Jetz et al., 2008; Lechki & Benson, 2026). Body size may further modulate Ashmole's mechanism, as the higher adult survival of larger birds could buffer mortality-driven population declines during seasonal resource minima (Scholer et al., 2020). How reproductive investment is partitioned among offspring provides a second constraint, as greater investment in egg mass generally trades off against offspring number (Lack, 1967; Martin et al., 2006; Smith & Fretwell, 1974). Migration adds a temporal dimension to this energetic framework. Migratory mortality can favour faster life histories and greater reproductive allocation, while seasonal movements allow species to escape resource minima and track resource pulses, potentially reducing their exposure to the resource bottlenecks

central to Ashmole's mechanism (Lundblad & Conway, 2021; Soriano-Redondo et al., 2020; Winger & Pegan, 2021).

Recent advances in phylogenetic comparative methods have enabled explicit tests of how intrinsic and environmental factors shape trait evolution by modelling heterogeneity in evolutionary dynamics across lineages. Variable-rates models identify lineage-specific shifts in evolutionary rates (Venditti et al., 2011), while the new Fabric model extends this framework by jointly estimating variation in evolutionary rates and directional shifts in trait evolution (Pagel et al., 2022). Within a phylogenetic regression framework, these models allow predictors to be associated with specific evolutionary events across the tree, identifying whether lineages experienced changes in evolvability, directionality, or both (Baker et al., 2015a; Baker & Venditti, 2019; Furness et al., 2022; Pagel & Meade, 2025).

Passeriformes provide a particularly suitable group for examining how climatic seasonality has shaped clutch-size evolution because they encompass extensive evolutionary variation in clutch size (Pienaar et al., 2013), migratory strategy and climatic exposure (Eyres et al., 2020), within a broadly comparable altricial reproductive framework (Ducatez & Field, 2021). This restriction is particularly useful because developmental mode itself is a major determinant of reproductive output across birds, affecting both clutch size and its scaling with body mass (Lechki & Benson, 2026). Moreover, unlike several other passerine reproductive traits, clutch size shows little phylogenetic inertia and appears able to respond rapidly to changing climatic regimes (Pienaar et al., 2013).

To characterise the seasonal resource environment experienced by species, we use actual terrestrial evaporation (Or evapotranspiration), which integrates water and energy availability and is closely associated with terrestrial primary productivity (Lundblad & Conway, 2021). Rather than collapsing seasonality into a single index, we describe the annual resource cycle through its minimum (Emin) and maximum (Emax), thereby separating the severity of the resource bottleneck from the magnitude of subsequent resource availability. These two components correspond directly to the demographic mechanism Ashmole proposed.

Hypothesis

We hypothesise that seasonal resource limitation, acting through the demographic processes Ashmole proposed, has shaped the latitudinal gradient in passerine clutch size over evolutionary time by altering the direction and tempo of clutch size evolution across lineages. Intrinsic life-history traits that modify exposure to seasonal resource bottlenecks or reproductive allocation may modulate this process.

Predictions

I. Species experiencing greater seasonal contrasts in resource availability should have larger mean clutch sizes.

II. Mean clutch size should decrease as minimum resource availability (Emin) increases, consistent with weaker demographic bottlenecks under less limiting conditions.

III. Minimum resource availability (Emin) should have a stronger influence on interspecific variation in clutch size than maximum resource availability (Emax).

IV. Climate–clutch size relationships should be weaker in larger-bodied and migratory species, which are expected to be buffered against seasonal resource bottlenecks, and in species producing relatively larger eggs, for which greater per-offspring investment may constrain the extent to which seasonal resource pulses can be translated into increased offspring number.

V. Larger-bodied, migratory species, and species producing relatively larger eggs should show fewer and/or weaker climate-associated shifts in evolutionary direction and tempo, reflecting either reduced exposure to seasonal resource bottlenecks or stronger energetic constraints on the evolutionary response of clutch size.

OBJECTIVES

GENERAL OBJECTIVE

To evaluate the predictions of Ashmole's hypothesis at a macroevolutionary scale by testing whether seasonal resource limitation is associated with interspecific variation in passerine clutch size, lineage-specific changes in its evolutionary direction and evolvability, and differential responses among species with contrasting phenotypic traits and life-history strategies.

SPECIFIC OBJECTIVES

1. To test the predicted relationships between clutch size and seasonal resource availability by jointly estimating the effects of minimum (Emin) and maximum (Emax) actual terrestrial evaporation, their interaction, and the relative contribution of each climatic component.
2. To determine whether body mass, egg mass and migratory strategy modify the relationship between seasonal resource availability and clutch size, while accounting for phylogenetic non-independence.
3. To characterise heterogeneity in the evolutionary direction and evolvability of clutch size across the passerine phylogeny and identify the evolutionary changes associated with climatic seasonality relative to those associated with body mass, egg mass and migration.

4. To test whether the frequency and magnitude of climate-associated directional and evolvability shifts accumulated along lineages vary among climatic zones and by body mass, egg mass, and migratory strategy.

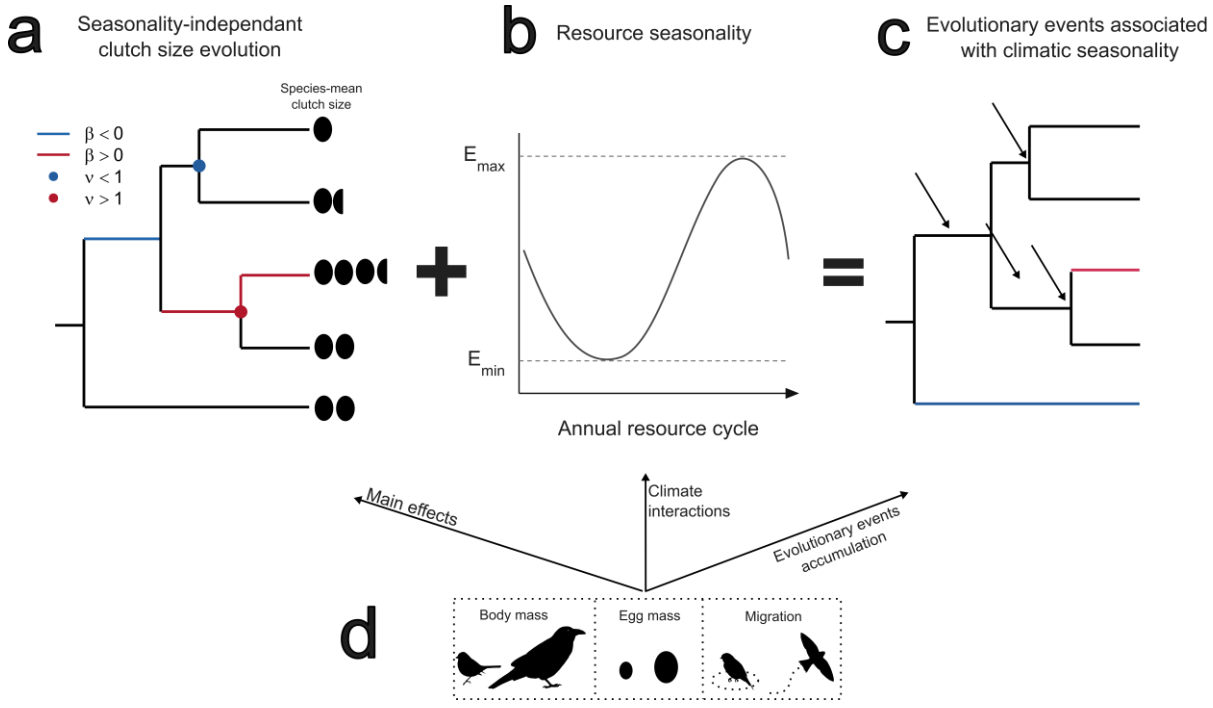

Figure 2. Conceptual framework for identifying the effects of climatic seasonality on clutch-size macroevolution. **a**, Species-mean clutch-size evolution is first modelled across the phylogeny while accounting for covariate effects unrelated to climatic seasonality. The most complex evolutionary model considered, Fabric, allows lineage-specific changes in both evolutionary direction (β) and evolvability (v). The variable-rates model is the simpler alternative, allowing only shifts in evolvability. **b**, Climatic seasonality is then incorporated using the mean minimum and maximum annual actual evaporation experienced across each species' habitat (Emin and Emax), allowing their individual effects and interaction to describe variation across the annual resource cycle. **c**, Comparison of models with and without the climatic component identifies

how seasonal resource limitation reorganises the inferred evolutionary history. Events that lose support after Emin and Emax are included are operationally classified as associated with climatic seasonality (i.e climate-associated); events retained in both models are not classified as climate-associated; and additional events may become supported only after incorporating climatic seasonality. **d**, Body mass, egg mass and migration are incorporated as allometric and life-history covariates to test three complementary components: (i) their main effects on species-mean clutch size, (ii) their potential interactions with climatic seasonality, and (iii) their association with the frequency and magnitude of climate-associated evolutionary events accumulated along lineage histories.

METHODS

Life-history data and climatic variables

We analysed clutch-size evolution across Passeriformes. We obtained life-history data primarily from BIRDBASE v2025.1 (Şekercioğlu et al., 2025), with species names standardised to the eBird/Clements Checklist v2024. Clutch size was taken directly when a mean was reported and otherwise calculated as the midpoint of the reported minimum and maximum. Mean adult body mass was obtained from BIRDBASE, and mean egg mass from Rotenberry and Balasubramaniam (2020) empirical measurements only, to avoid introducing body-mass-derived values as an independent predictor. We excluded species associated primarily with marine or coastal environments and island-restricted species because the climatic data described terrestrial conditions. The resulting dataset contained 1,938 species before phylogenetic pruning.

Species distributions were obtained from BirdLife International Area of Habitat maps v2023.1. We calculated climatic variables from the resident area of habitat distributions for resident species and from breeding distributions for migrants, describing conditions where most populations reproduce. We followed the migratory classification provided by BirdLife International/IUCN: species mapped with breeding ranges were classified as migratory, whereas species mapped with resident ranges were classified as resident; we did not use non-breeding

distributions. After excluding Area of Habitat values <0.1 (less than 10% of that area was suitable habitat), we sampled 500 locations per species with replacement, weighted by habitat suitability values, and averaged environmental conditions across these samples.

Seasonal conditions were characterised using actual terrestrial evaporation (E; “actual evaporation” in GLEAM; or evapotranspiration) from GLEAM v4.2a (Miralles et al., 2025), at 0.1° resolution for 1980–2024. For each grid cell, we calculated a 12-month climatology across the 45-year period and defined Emax and Emin as the maximum and minimum monthly values, respectively. Species-level values were averaged across the sampled resident or breeding distribution. We treated evaporation as a proxy for seasonal terrestrial water–energy conditions and vegetation activity rather than direct food abundance. We modelled Emin and Emax separately and through their interaction, allowing us to distinguish the severity of the annual resource minimum and subsequent resource availability rather than impose a predefined seasonality index/ratio (Hořák et al., 2015; Lundblad & Conway, 2021).

Phylogenetic framework

We used the time-calibrated AvesTree v1.5 phylogeny (McTavish et al., 2025), pruned to the species represented in the complete dataset. We then removed phylogenetically redundant observations using the unique-data pruning

procedure in FabricTools, which retains a single representative from clades with identical clutch-size values. This reduced the final dataset from 1,938 to 1,663 species, and we used the resulting dated phylogeny for all evolutionary and lineage-level analyses.

Phylogenetic modelling of clutch-size evolution

Clutch size, body mass, egg mass, Emax and Emin were log10-transformed, and continuous predictors were mean-centred. We coded migration as resident (0) or migrant (1). The initial regression included body mass, egg mass, Emax, Emin, and migration, along with all two-way interactions. We simplified this structure separately under Brownian motion, Variable Rates and Fabric by sequentially removing the least-supported interaction while retaining all main effects (Bayesian Stepwise regression). Simplification ceased when each remaining interaction had at least 95% of its posterior distribution on one side of zero.

The three evolutionary models represent progressively more heterogeneous descriptions of residual clutch-size evolution. Brownian motion assumes a single evolutionary variance across the phylogeny. Variable Rates allows this background variance to be modified locally by rate scalars, with values >1 indicating faster and values <1 slower evolution; rate changes can affect individual branches or descendant clades (Baker et al., 2015b; Venditti et al., 2011). Fabric additionally distinguishes changes in evolutionary direction from changes in

evolvability. Directional effects (β) occur along branches and describe sustained change towards larger or smaller clutch sizes, whereas evolvability scalars (v) arise at ancestral nodes and modify the Brownian variance inherited by descendant lineages (Pagel & Meade, 2025; Pagel et al., 2022). Both processes are estimated jointly with the regression coefficients and therefore describe evolutionary departures remaining after accounting for the included predictors.

We ran stepwise regressions for 100 million iterations, discarding the first 12.5 million as burn-in and sampling every 50,000 iterations. We assigned normal priors to the regression coefficients with mean 0 and standard deviation 3. We inspected posterior traces and effective sample sizes to assess convergence. We compared the final Brownian, Variable-Rates, and Fabric regressions using marginal likelihoods estimated by stepping-stone sampling with 1,000 stones and 10,000 iterations per stone. Bayes factors were calculated as twice the difference in log marginal likelihood (2ΔlogML), with values of 0–2, 2–5, 5–10 and >10 interpreted as weak, positive, strong and very strong evidence, respectively. We then replicated the best-supported model across six independent MCMC runs to assess the consistency of inferred evolutionary events; we retained only events supported across all six runs for subsequent analyses.

Posterior predictions from the selected Fabric regression were used to describe the conditional relationship between Emin and Emax and clutch size. We evaluated each climatic predictor at the 10th percentile, median, and 90th

percentile of the others, with continuous covariates at their centred means; we then transformed predictions back to the original clutch-size scale.

Predictor contributions to macroevolutionary events

We quantified the contribution of individual predictors by refitting the selected Fabric regression after removing each predictor in turn, along with any interaction involving that predictor, and fitted a model excluding Emin, Emax, and their interaction jointly. We ran reduced Fabric models for 400 million iterations, discarded 50 million as burn-in, and sampled every 200,000 iterations. We measured each predictor's contribution to interspecific variation from the posterior difference in phylogenetic R^2 between the full and corresponding reduced regression.

We then used the same comparisons to identify the evolutionary changes associated with each predictor. Following the logic used to identify ecological drivers of exceptional evolutionary rates (Baker & Venditti, 2019; Furness et al., 2022), a directional or evolvability shift supported in a reduced model but no longer supported after the predictor was included was operationally classified as associated with that predictor (Pagel & Meade, 2025). Conversely, shifts retained in both models were not classified as predictor-associated, whereas shifts supported only after inclusion were recorded as newly supported evolutionary events. Baker and Venditti (2019) apply the same inferential logic, associating

ecological effects with rapid evolutionary shifts when predictor inclusion removes residual rate shifts required by the simpler model. Fabric outputs from six independent runs were post-processed using FabricPostProcess and CombineFabric, and only events supported across all six runs were retained.

tip-level accumulation of climate-associated evolution

To test whether sensitivity to climatic selection differed among passerine phenotypes, we summarised the climate-associated evolutionary history leading to each species. Along each root-to-tip path, we counted positive directional shifts, negative directional shifts, their total absolute directional shifts, and evolvability shifts, and separately calculated the cumulative magnitude of each type of evolutionary change. We accumulated directional magnitudes separately by sign, expressing negative changes as absolute magnitudes when comparing their total contribution.

We classified species as tropical or temperate/polar based on mean absolute latitude, using the tropical boundary of 23.43587° (Drury et al., 2021). We then tested body mass, egg mass, migration, and climatic zone as predictors of the number and magnitude of climate-associated evolutionary changes accumulated along each lineage.

We analysed event counts using Bayesian phylogenetic Poisson regressions with a log link in brms (Bürkner, 2017). Models included body mass, egg mass,

migration and climatic zone, together with the logarithm of the number of root-to-tip branches as an offset, so coefficients describe variation in event frequency per evolutionary opportunity rather than differences in path length. We incorporated phylogenetic covariance as a species-level random effect. Models used four chains of 1,000 iterations, including 500 warm-up iterations, with normal(0,1) priors on regression coefficients, normal(-3,2) on the intercept and exponential(1) on the phylogenetic standard deviation; adapt_delta was 0.995 and max_treedepth 15. We evaluated sampling convergence using R-hat and effective sample sizes (>200). The final fitted models indeed contain all 1,663 species and use this Poisson formulation.

Because associations could differ among passerine radiations, we additionally fitted phylogenetic Poisson models including the six major passerine clades, as defined in the passerine classification provided by Bird Phylogeny (https://www.bird-phylogeny.de/superorders/australaves/passeriformes/), with sufficient representation: Tyranni, Meliphagides, Corvides, Sylviida, Muscicapida and Passerida (n = 1,624). All six clades were included simultaneously as levels of a categorical predictor, with clade × body mass, clade × egg mass and clade × migration interactions allowing the corresponding effects to vary among clades. Climatic zone was retained as a common effect, together with the root-to-tip branch offset and phylogenetic covariance structure. Smaller passerine clades were excluded because of insufficient representation (Menurides, n = 1;

Climacterides, n = 11; Orthonychides, n = 5; Picathartida, n = 15; Stenostiridae + Hyliotidae, n = 7), accounting for the 39 species omitted from these analyses.

We log10(x + 1)-transformed cumulative event magnitudes and analysed them across the complete phylogeny using Bayesian constant-rate phylogenetic regressions (Or PGLS) in BayesTraits, with body mass, egg mass, migration, and climatic zone as predictors. We ran these models for 10 million iterations, discarding 2 million as burn-in and sampling every 8,000 iterations, with normal(0,3) coefficient priors. We did not repeat magnitude models within clades because several clades had insufficient within-clade variation in these continuous evolutionary histories for stable inference.

RESULTS

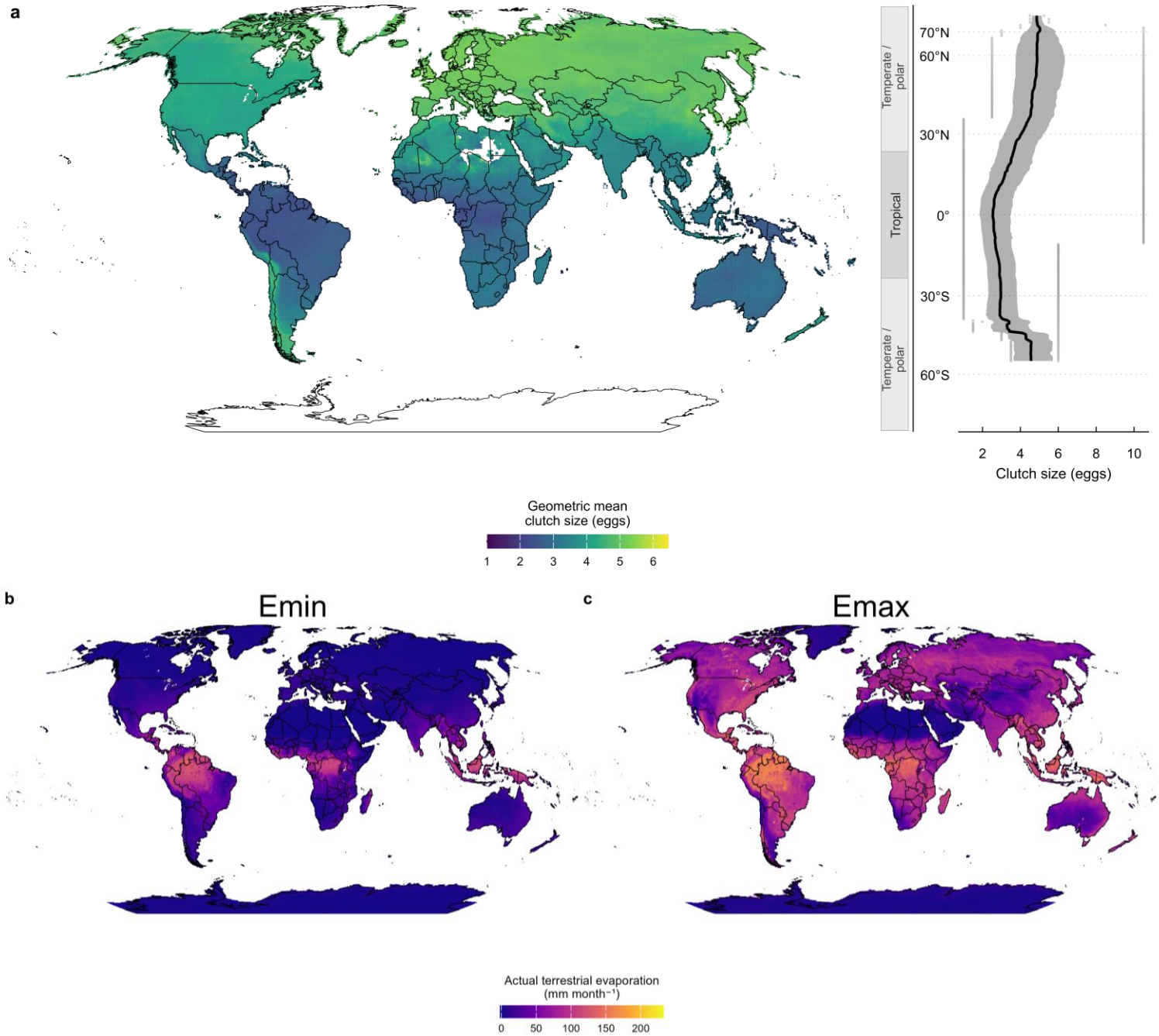
a
Temperate / polar
Tropical
Temperate / polar
70°N
60°N
30°N
0°
30°S
60°S
2
4
6
8
10
Clutch size (eggs)
Geometric mean clutch size (eggs)
1
2
3
4
5
6
b
Emin
c
Emax
Actual terrestrial evaporation (mm month⁻¹)
0
50
100
150
200

Figure 3. Global patterns of passerine clutch size and seasonal resource availability. a, Geometric mean clutch size across 50-km grid cells, with the latitudinal profile showing the mean (black line), ±1 geometric SD (grey band) and observed minima and maxima (grey points). **b–c,** Global distributions of minimum (Emin) and maximum (Emax) monthly actual terrestrial evaporation, respectively, shown on a common scale (mm month^{-1}).

Among the evolutionary models evaluated, the Fabric regression was the best-supported model, outperforming both the variable-rates model (Bayes factor = 207.93) and the homogeneous Brownian-motion model (Bayes factor = 767.61; Supplementary Table S7). The variable-rates model was also strongly preferred over Brownian motion (Bayes factor = 559.68). Stepwise Bayesian model simplification produced a final Fabric regression in which the interaction between Emin and Emax was the only supported two-way interaction (b = -0.115, PMCMC < 0.05; Supplementary Table S4).

Clutch size decreased with increasing Emin, with higher Emax accentuating this negative relationship (Figure 4). At average Emax, a tenfold increase in Emin was associated with a 21% decrease in clutch size (b = -0.100, 90% CrI [-0.112, -0.088], PMCMC < 0.05). Emax, in contrast, showed no detectable association with clutch size at average Emin (b = -0.019, 90% CrI [-0.058, 0.022], PMCMC > 0.05), but instead modulated the strength of the negative relationship with Emin. Clutch size was also positively associated with body mass (b = 0.136, 90% CrI [0.080, 0.189]; Figure 5a) and migration (b = 0.062, 90% CrI [0.051, 0.073]; Figure

5c) and negatively associated with egg mass (b = -0.195, 90% CrI [-0.271, -0.119]; Figure 5b).

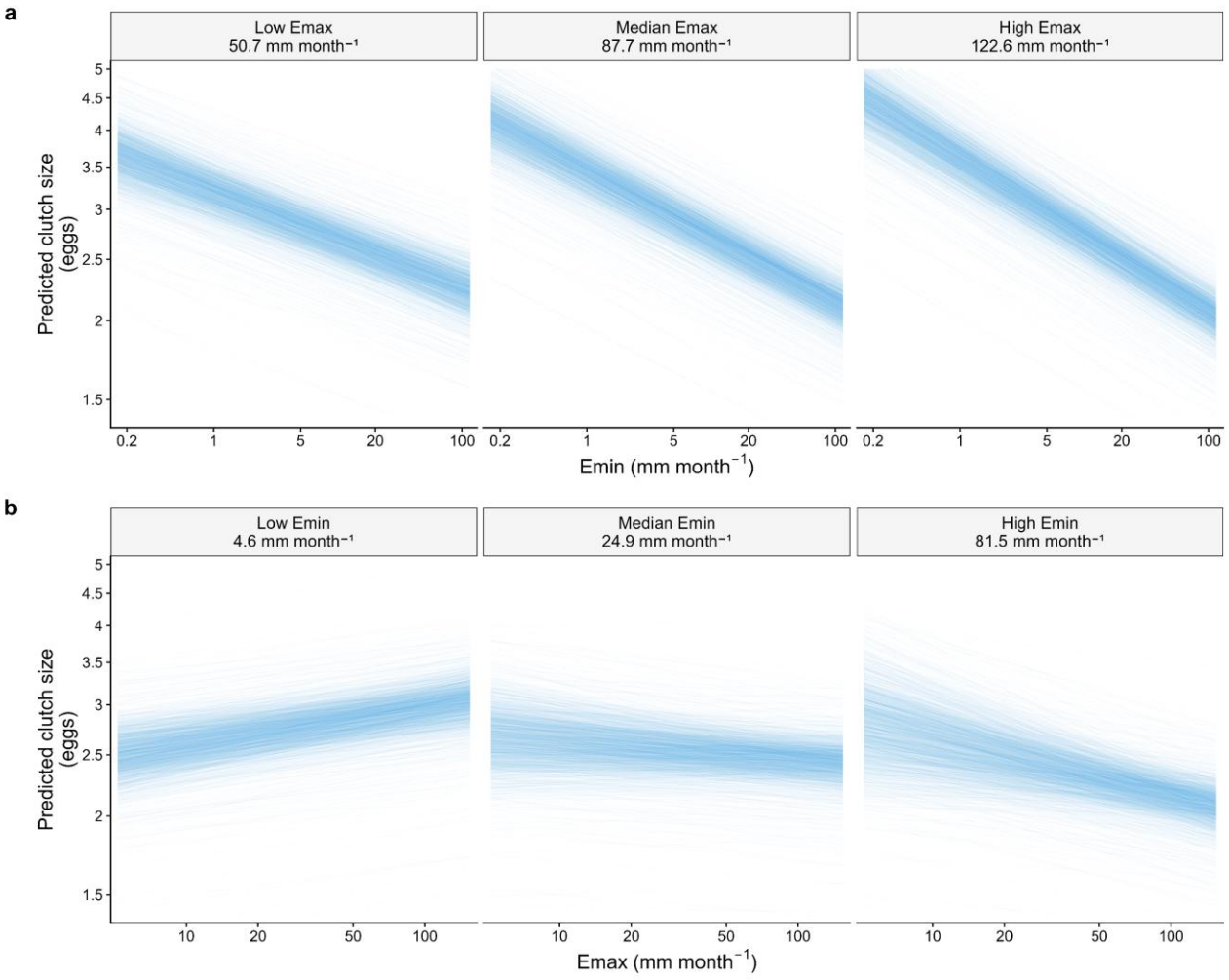

Figure 4. Conditional effects of minimum (Emin) and maximum (Emax) resource availability on avian clutch size. a, Predicted effect of minimum actual evaporation (Emin) on clutch size, conditional on Emax fixed at its 10th percentile, median and 90th percentile. **b**, Predicted effect of maximum actual evaporation (Emax) on clutch size, conditional on Emin fixed at the same three

levels. Each light-blue line represents the prediction from one of the 1,751 posterior samples. Predictions correspond to resident species, with body mass and egg mass held at their centred means. Values above each facet indicate the fixed climatic condition in mm month^{-1}. Differences in slopes among facets represent the estimated Emin × Emax interaction. Both climatic predictors and clutch size were modelled on the $\log_{10}$ scale, but axes are labelled in their original units of mm month^{-1} and number of eggs, respectively.

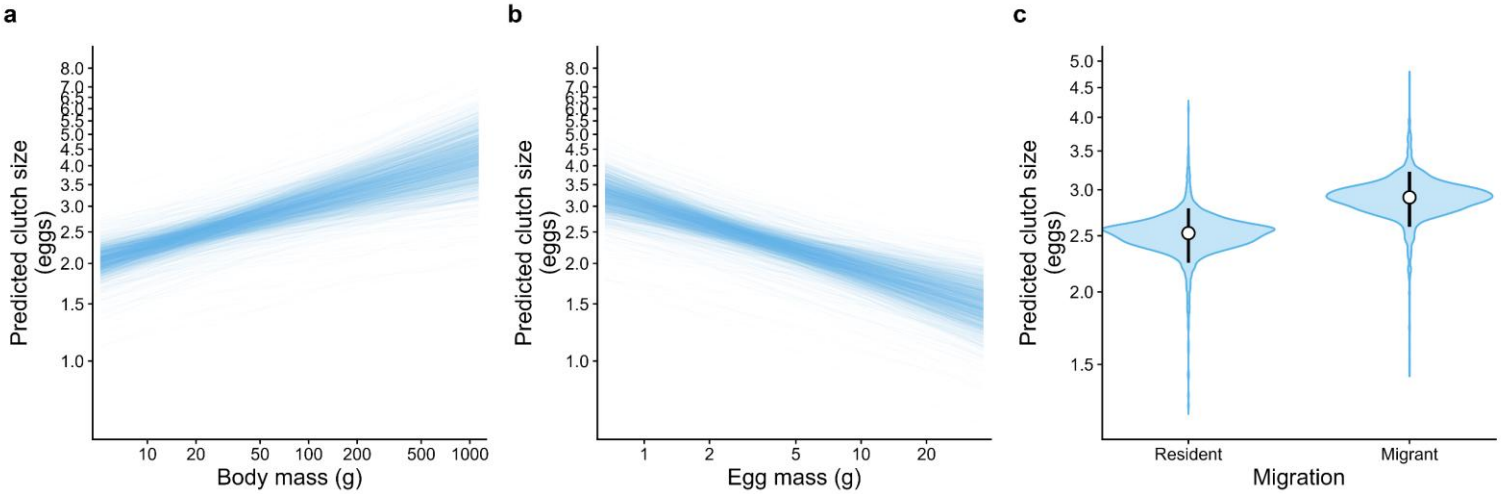

Figure 5. Effects of body mass, egg mass and migration on avian clutch size. a, b, Posterior predictions across body mass and egg mass; light-blue lines represent posterior draws, with other predictors held at their centred means. **c**, Posterior distributions for resident and migratory species; points show posterior medians and bars 90% credible intervals. Body mass and egg mass are shown in grams. No interactions involving body mass, egg mass or migration were retained in the final model.

The climatic component contributed 18.0% (Table 1) of the interspecific variation in clutch size. This contribution was driven predominantly by Emin, which

contributed 14.2% (Table 1) of the variation, approaching four-fifths of the total climatic contribution. In comparison, Emax and the Emin × Emax interaction contributed 2.3% and 1.7%, respectively (Table 1). Thus, although the interaction showed that Emax modified the relationship between Emin and clutch size, minimum resource availability contributed most of the climate-associated reduction in R^2. Among the non-climatic predictors, migration contributed the most. Despite its modest positive effect on clutch size (b = 0.062, Figure 5), migration contributed 5.6% of the interspecific variation, exceeding the contributions of the allometric life-history predictors, body mass and egg mass, which contributed 1.6% and 1.8%, respectively. The complete model (including all retained predictors) had a posterior R^2 of 37.5%.

Table 1. Contributions of predictors to interspecific variation in clutch size. Values are posterior median reductions in R^2 after excluding each predictor from the complete Fabric regression, with 95% credible intervals.

Excluded predictor	Contribution to R^2 [95% CrI]
Emin, Emax and Emin × Emax excluded	0.180 [0.116, 0.258]
Emin excluded	0.142 [0.076, 0.226]
Migration excluded	0.056 [-0.041, 0.144]
Emax excluded	0.023 [-0.057, 0.102]
Egg mass excluded	0.018 [-0.068, 0.104]
Emin × Emax interaction excluded	0.017 [-0.066, 0.105]
Body mass excluded	0.016 [-0.094, 0.107]

Climatic seasonality, represented by Emin and Emax, was associated with 65 of 193 (33.7%) directional shifts and 47 of 219 (21.5%) evolvability shifts (Tables 2

and 4; Figure 6). Incorporating climatic seasonality also altered the set of evolutionary events supported across the phylogeny: 128 directional shifts were retained, whereas 58 additional shifts were supported only after climate was included. Climate-associated directional shifts showed no overall bias, comprising 32 increases and 33 decreases in clutch size. For evolvability, we retained 172 shifts, and 71 additional shifts were supported after incorporating climate. Notably, all 47 climate-associated evolvability shifts represented increases in evolutionary rate (scalar > 1).

The climatic signal was concentrated primarily in Emin, which was associated with 60 directional shifts (29.6%) and 51 evolvability shifts (22.6%), compared with only 9 (5.1%) and 26 (10.3%), respectively, for Emax. The Emin × Emax interaction was associated with a further 16 directional shifts (9.0%) and 20 evolvability shifts (8.1%) (Tables 2 and 4).

Among non-climatic predictors, migration was associated with the largest number of evolutionary events: 32 directional shifts (17.5%) and 35 evolvability shifts (15.3%), exceeding the corresponding numbers associated with body mass and egg mass (Tables 2 and 4). Notably, migration was the only predictor associated with an evolvability decrease below Brownian expectations ($v < 1$), localised to the ancestral branch subtending six migratory *Phylloscopus* species (Phylloscopidae), with clutch sizes ranging from 4.5 to 6 eggs. Thus, despite its comparatively modest association with mean clutch size, migration was more

strongly associated with lineage-specific changes in both evolutionary direction and evolvability than either allometric trait.

Table 2. Directional shifts associated with predictor inclusion.

		>0		<0		
Predictor	**Reduced-model shifts**	**Events, n (%)**	**Median magnitude**	**Events, n (%)**	**Median magnitude**	**Total, n (%)**
Emin	203	26 (12.8%)	0.189	34 (16.7%)	-0.191	60 (29.6%)
Emax	175	2 (1.1%)	0.173	7 (4%)	-0.195	9 (5.1%)
Body mass	181	9 (5%)	0.0779	8 (4.4%)	-0.189	17 (9.4%)
Egg mass	181	8 (4.4%)	0.173	10 (5.5%)	-0.195	18 (9.9%)
Migration	183	11 (6%)	0.189	21 (11.5%)	-0.192	32 (17.5%)
Emin + Emax	193	32 (16.6%)	0.194	33 (17.1%)	-0.199	65 (33.7%)
Emin × Emax interaction	178	9 (5.1%)	0.137	7 (3.9%)	-0.177	16 (9%)

Note: Shifts supported in the reduced model (without a predictor) but no longer supported after inclusion of the predictor in the complete model. Percentages are relative to the total number of directional shifts in the corresponding reduced model. Median magnitude is the median absolute branch-scaled directional effect, calculated separately for positive and negative shifts. The complete model contained 186 directional shifts.

Table 3. New directional shifts supported after predictor inclusion.

	>0		<0		
Predictor	**Events, n (%)**	**Median magnitude**	**Events, n (%)**	**Median magnitude**	**Total, n (%)**
Emin	19 (10.2%)	0.192	24 (12.9%)	0.185	43 (23.1%)
Emax	10 (5.4%)	0.195	10 (5.4%)	0.184	20 (10.8%)
Body mass	9 (4.8%)	0.192	13 (7%)	0.18	22 (11.8%)
Egg mass	8 (4.3%)	0.174	15 (8.1%)	0.182	23 (12.4%)
Migration	17 (9.1%)	0.182	18 (9.7%)	0.196	35 (18.8%)
Emin + Emax	29 (15.6%)	0.192	29 (15.6%)	0.184	58 (31.2%)
Emin × Emax interaction	11 (5.9%)	0.192	13 (7%)	0.193	24 (12.9%)

Note: Shifts supported in the complete model but not when the predictor was excluded. Percentages are relative to the 186 directional shifts in the complete model. Median magnitude is the median absolute branch-scaled directional effect from the complete model, calculated separately for positive and negative shifts.

Table 4. Evolvability shifts associated with predictor inclusion.

		>1		<1		
Predictor	**Reduced-model shifts**	**Events, n (%)**	**Median magnitude**	**Events, n (%)**	**Median magnitude**	**Total, n (%)**
Emin	226	51 (22.6%)	5.34	0 (0%)	-	51 (22.6%)
Emax	252	26 (10.3%)	5.01	0 (0%)	-	26 (10.3%)
Body mass	240	22 (9.2%)	4.69	0 (0%)	-	22 (9.2%)
Egg mass	245	25 (10.2%)	4.73	0 (0%)	-	25 (10.2%)

Predictor	Reduced-model shifts	>1		<1		Total, n (%)
		Events, n (%)	Median magnitude	Events, n (%)	Median magnitude	
Migration	229	34 (14.8%)	5.5	1 (0.4%)	0.242	35 (15.3%)
Emin + Emax	219	47 (21.5%)	4.94	0 (0%)	-	47 (21.5%)
Emin × Emax interaction	248	20 (8.1%)	4.72	0 (0%)	-	20 (8.1%)

Note: Shifts supported in the reduced (without a predictor) model but no longer supported after inclusion of the predictor in the complete model. Percentages are relative to the total number of evolvability shifts in the corresponding reduced model. Median magnitude is the median evolvability scalar, calculated separately for increases (>1) and decreases (<1) in evolvability. The complete model contained 243 evolvability shifts.

Table 5. New evolvability shifts supported after predictor inclusion.

Predictor	>1		<1		Total, n (%)
	Events, n (%)	Median magnitude	Events, n (%)	Median magnitude	
Emin	67 (27.6%)	5.15	1 (0.4%)	0.236	68 (28%)
Emax	16 (6.6%)	5.21	1 (0.4%)	0.236	17 (7%)
Body mass	25 (10.3%)	4.97	0 (0%)	-	25 (10.3%)
Egg mass	23 (9.5%)	4.96	0 (0%)	-	23 (9.5%)
Migration	49 (20.2%)	5.11	0 (0%)	-	49 (20.2%)
Emin + Emax	70 (28.8%)	5.21	1 (0.4%)	0.236	71 (29.2%)
Emin × Emax interaction	15 (6.2%)	5.34	0 (0%)	-	15 (6.2%)

Note: Shifts supported in the complete model but not when the predictor was excluded. Percentages are relative to the 243 evolvability shifts in the complete model. Median magnitude is the median complete-model evolvability scalar, calculated separately for increases (>1) and decreases (<1) in evolvability.

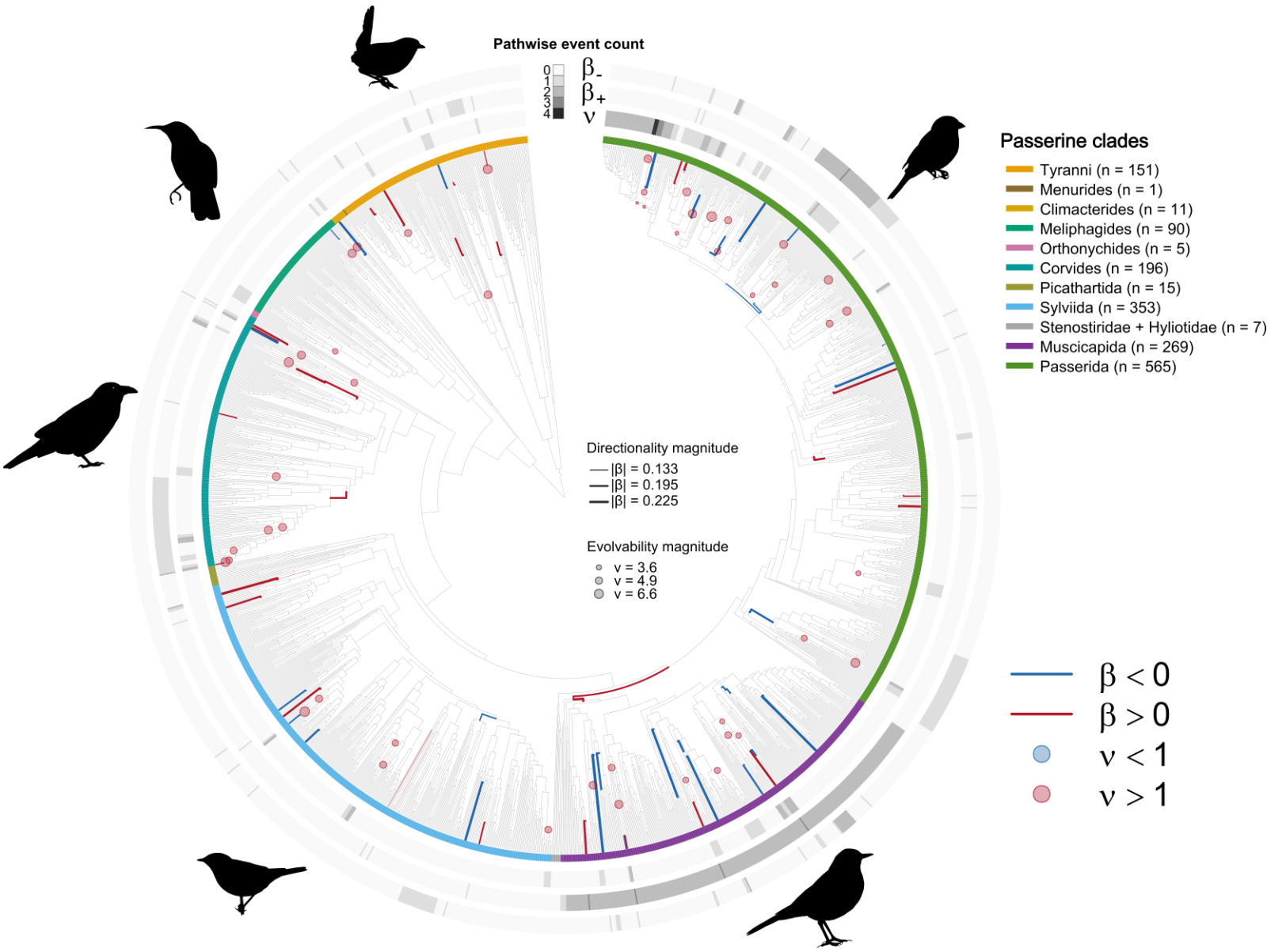

Figure 6. Phylogenetic distribution of evolutionary events associated with climatic seasonality. Evolutionary events associated with Emin and Emax are mapped across the passeriform phylogeny. Red and blue branches indicate positive and negative directional shifts in clutch-size evolution, respectively, with branch width proportional to the magnitude of the directional effect (|β × BL|). Circles indicate shifts in evolvability (v); red and blue denote increases (v > 1) and decreases (v < 1), respectively, and circle size is proportional to the estimated

evolvability scalar. The three inner rings show the number of climate-associated events accumulated along each root-to-tip path, separately for evolvability shifts (v), positive directional shifts (β+) and negative directional shifts (β−). The outermost coloured ring identifies the major Passeriformes clades represented in the phylogeny; silhouettes obtained from PhyloPic.com mark the six clades included in the post-hoc analyses (Tyranni, Meliphagides, Corvides, Sylviida, Muscicapida and Passerida).

Climate-associated directional evolution differed markedly across climatic zones. Temperate and polar lineages accumulated positive shifts at a 31% higher rate (Poisson model b = 0.27, 95% CrI [0.02, 0.53]) and negative shifts at a 70% lower rate (Poisson model b = -1.22, 95% CrI [-1.72, -0.74]) than tropical lineages, consistent with opposing historical tendencies towards larger and smaller clutches, respectively. Climatic zone was unrelated to the total accumulation of directional or evolvability shifts, while body mass, egg mass and migration showed no phylogeny-wide associations with event accumulation (Supplementary Table S1).

Migration showed clade-specific associations with climate-associated directional evolution. Resident lineages had substantially more positive climate-associated shifts than migrants in both Sylviida and Passerida. Relative to residents, migrants showed an 85% lower frequency of positive shifts in Sylviida (Poisson model b = -1.91, 95% CrI [-3.50, -0.61]) and a 76% lower frequency in Passerida (Poisson model b = -1.41, 95% CrI [-2.86, -0.21]). In Passerida, migrants also showed a 58% lower frequency of total directional shifts (Poisson model b = -0.87, 95% CrI

[-1.31, -0.44]), whereas egg mass was positively associated with total directional shifts (Poisson model b = 1.63, 95% CrI [0.09, 3.14]). We detected no within-clade associations for climate-associated evolvability shifts (Supplementary Table S2).

The accumulated magnitude of climate-associated directional change showed a similar pattern. Temperate and polar lineages accumulated greater positive directional change (b = 0.0040, 95% HPD [0.0028, 0.0055]) and less negative directional change (b = -0.0031, 95% HPD [-0.0047, -0.0016]) than tropical lineages. Resident lineages likewise accumulated greater positive directional change than migrants across the phylogeny (b = -0.0019, 95% HPD [-0.0036, -0.0005]). No associations were detected with total directional magnitude or accumulated evolvability, and neither body mass nor egg mass was associated with any pathwise magnitude measure (Supplementary Table S3).

DISCUSSION

Climate and clutch-size macroevolution

Our results identify seasonal resource limitation as a major correlate of clutch-size macroevolution across Passeriformes. Among the environmental and life-history factors examined, the climate block (both Emin and Emax) made the largest contribution to interspecific variation in clutch size, despite the high lability of this reproductive trait and its capacity to vary within females among breeding attempts as environmental conditions change (Chik et al., 2022; Hidalgo Aranzamendi et al., 2019; Martin et al., 2025). Previous comparative studies have repeatedly linked larger clutches to greater environmental seasonality (Griebeler et al., 2010; Hořák et al., 2015; Jetz et al., 2008); our results extend this pattern by showing that seasonal resource limitation is also associated with the macroevolutionary dynamics of clutch size across the passerine phylogeny.

The strong support for Fabric over both variable-rates and homogeneous Brownian models further indicates that clutch-size evolution cannot be characterised solely by heterogeneity in evolutionary rate. Instead, recurrent directional shifts were a prominent component of its macroevolutionary history, representing episodes in which lineages evolved towards larger or smaller clutch sizes beyond the expectation of a directionless Brownian process. In biological

terms, such shifts are consistent with repeated changes in lineage-specific reproductive optima as selective environments changed through evolutionary time (Pagel & Meade, 2025). Climatic seasonality was associated with 33.7% of these directional shifts, consistent with seasonal resource limitation repeatedly altering the selective context determining optimal reproductive investment and thereby favouring evolutionary shifts towards larger or smaller clutch sizes. Changes in evolvability constituted a second, distinct component of this history, and 21.5% of these shifts were likewise associated with the climatic block. Because directional and evolvability shifts represent statistically distinct macroevolutionary processes (Pagel & Meade, 2025), these results suggest that seasonal resource limitation is associated not only with where clutch size has evolved, but also with changes in its realised capacity to explore phenotypic space over evolutionary time.

The climatic signal was strongly asymmetric across the annual resource cycle. Minimum resource availability (Emin) accounted for most of the climatic contribution to interspecific variation and was associated with substantially more evolutionary events than maximum availability. Crucially, higher maximum resources (Emax) were associated with larger clutches only when annual minima were sufficiently low (i.e. higher seasonality). Severe resource bottlenecks are expected to reduce population density, increasing resources per breeder when conditions subsequently improve. As minima became less limiting, this demographic advantage disappeared, and the relationship with Emax ultimately

reversed, consistent with higher survival maintaining denser populations and lower per-capita resource availability during breeding (Ashmole, 1961; Ashmole, 1963; Hořák et al., 2015; Lundblad & Conway, 2021). This interaction indicates that the relationship with productive periods depends on the severity of the preceding resource bottleneck. Environments with similar overall seasonality can therefore impose very different demographic pressures if their annual minima differ. This distinction is lost when seasonality is summarised as a range or dispersion measueres, because environments with similar seasonal contrasts can differ fundamentally in the severity of their resource minima.

Our results are consistent with the latitudinal gradient in clutch size reflecting contrasting histories of directional evolution across climatic zones. Climate-associated shifts occurred in both tropical and temperate–polar lineages but differed in polarity: temperate and polar lineages were repeatedly biased towards larger clutches, whereas tropical lineages more often shifted towards smaller clutches. Under Ashmole's mechanism, strong seasonal bottlenecks outside the tropics reduce population density and increase per-capita resource availability when conditions subsequently improve, favouring greater reproductive investment (Ashmole, 1961; Ashmole, 1963; Ricklefs, 2000).

Low tropical fecundity need not represent an absence of strong climatic selective pressures for greater reproductive output, but an alternative adaptive route for allocating reproduction. Indeed, the deep evolutionary history of birds shows that reduced offspring number is itself a derived component of avian reproduction:

non-avian dinosaurs generally produced relatively large clutches of small eggs, whereas the bird-like strategy of fewer, larger offspring evolved later along the avian lineage (Lechki & Benson, 2026). Within modern birds, selection can further favour smaller clutches through greater investment in individual offspring (Martin, 2015) or by distributing reproductive effort among repeated breeding attempts (i.e. bet-hedging) (Griebeler & Böhning-Gaese, 2004; Griebeler et al., 2010; Liu et al., 2018; Song et al., 2020). The predominance of negative climate-associated shifts in tropical lineages therefore suggests that the latitudinal gradient reflects selection acting in both directions: towards greater investment per breeding attempt where seasonal demographic bottlenecks are strong, and towards alternative allocations of reproductive effort where they are weak.

Allometric constraints on reproductive allocation

Body mass and egg mass define a second axis of clutch-size variation that appears largely distinct from the climatic processes shaping its broad-scale evolutionary pattern. Egg mass was negatively associated with clutch size, consistent with the fundamental trade-off between offspring size and number. The positive association with body mass initially appears inconsistent with Calder's rule and with the decline in mass-specific reproductive production expected with increasing body size (Boyer et al., 2010; Calder, 1984). However, our estimate is conditional on egg mass and therefore describes variation in clutch size among

passerines for a given level of investment per egg, rather than conventional bivariate allometry. This distinction is consistent with the evolutionary interdependence of body size, offspring size and offspring number (Lechki & Benson, 2026).

At the scale of the whole phylogeny, neither body nor egg mass substantially altered the climatic response of clutch size or consistently predicted the accumulation of climate-associated evolutionary change, suggesting that their principal influence lies in reproductive allocation rather than climatic sensitivity. The clade-specific pattern in Passerida, however, indicates that this relationship is not purely constraining: lineages investing more heavily in individual offspring also accumulated more directional changes in clutch-size evolution (Supplementary Table S2). This suggests that the offspring size–number trade-off may itself shape the evolutionary flexibility of reproductive allocation, with some radiations repeatedly adjusting offspring number while maintaining comparatively high investment per offspring. Rather than imposing a uniform constraint on clutch-size evolution within Passerida, greater egg investment may be associated with alternative evolutionary routes through which reproductive effort is redistributed between offspring size and number.

Similar climatic responses, divergent evolutionary histories

Migration reveals that similar climate–clutch size relationships can arise through different evolutionary histories. Migrants and residents responded similarly to

climatic seasonality (Supplementary Table S4), despite differing in how clutch size evolved along their lineages. Across the phylogeny, resident lineages accumulated stronger climate-associated evolutionary increases in clutch size, while within Sylviida and Passerida migrants experienced fewer evolutionary shifts towards larger clutches (Supplementary Tables S2–S3). Migration therefore appears to alter how climatic pressures are translated into long-term changes in reproductive investment without substantially changing the contemporary relationship between climate and clutch size.

This decoupling is consistent with the equal fitness paradigm, in which alternative life-history strategies can achieve comparable fitness through different combinations of reproduction and survival (Brown et al., 2018). Residents are continuously exposed to local seasonal resource minima, whereas migrants can track seasonal environments and thereby alter the timing and intensity of exposure to resource bottlenecks, while simultaneously incurring the demographic costs and constraints of migration (Bell et al., 2024; Martin et al., 2023; Varpe, 2017; Winger & Pegan, 2021). Across birds, migration is associated with shifts in the balance between reproduction and survival, although the direction of these shifts can vary with migratory strategy and distance (Soriano-Redondo et al., 2020; Winger & Pegan, 2021). Migration therefore imposes its own demographic and energetic pressures, potentially providing an alternative route through which reproductive investment evolves.

Migrants and residents may consequently reach similar climate–clutch size relationships through different demographic routes: residents through repeated exposure to local seasonal resource bottlenecks, and migrants through a distinct combination of seasonal resource tracking and migration-related life-history pressures.

Origins and dimensions of clutch-size variation

Climatic seasonality was also consistently associated with shifts in the tempo of clutch-size evolution (Table 4). These climate-associated accelerations were substantial, with evolutionary rates typically approaching five times the Brownian background rate. Yet these accelerations did not accumulate preferentially in lineages differing in climatic zone, body mass, egg mass or migration, providing little evidence that the phenotypes examined here consistently differ in their sensitivity to climate-associated variation in evolvability. Climate-associated accelerations therefore occurred across a broad range of passerine lineages, rather than primarily within particular ecological or life-history groups.

Haywood (2013) argued that external selective pressures can influence the evolution of clutch size only through the developmental mechanisms that generate variation in egg number. In this framework, evolutionary changes in clutch size may arise through heterochronic changes in the number of pre-ovulatory follicles surviving follicular disruption or in the timing of the signal that

terminates follicular growth. Haywood further proposed that environmentally induced plasticity in these mechanisms could, under persistent selection, provide a route towards genetically assimilated differences among populations and species. This provides a plausible mechanistic substrate for the accelerations detected here: climatic selection may repeatedly favour changes in reproductive reaction norms, while developmental and regulatory differences determine how rapidly those responses become evolutionarily established. Evidence that clutch-size reaction norms vary among individuals and can themselves experience selection supports the first component of this pathway (Chik et al., 2022; Martin et al., 2025). Epigenetic regulation offers an additional, largely unexplored mechanism connecting environmental responsiveness with inherited reproductive differences. Genomic selection for avian laying date has already produced both genetic differentiation and changes in DNA methylation, including loci associated with reproductive and gonadal function (Lindner et al., 2024). Although this evidence concerns reproductive timing rather than clutch size directly, it demonstrates that avian reproductive traits can respond to selection through coupled genetic and epigenetic changes. Testing whether similar regulatory processes underlie clutch-size plasticity would directly link the macroevolutionary accelerations identified here to the developmental mechanisms proposed by Haywood.

Clutch size nevertheless captures only one component of reproductive strategy. Selection acts on combinations of offspring number, investment per offspring,

breeding frequency and survival, rather than on egg number in isolation (Pincheira-Donoso & Hunt, 2017). Our results suggest a hierarchical organisation of these processes: migration modifies the demographic route through which that environment is experienced, and body and egg size constrain the allocation of reproductive investment. By identifying resource minima as the principal climatic component, reconstructing climate-associated changes in evolutionary direction and tempo and showing that their historical accumulation differs among climatic zones and migratory strategies, our results document a cross-scale pattern compatible with Ashmole's population-level mechanism. Its macroevolutionary relevance would therefore arise not from a direct effect at the species level, but from the cumulative consequences of recurrent selection on reproductive allocation within populations. Demonstrating this pathway will require population-level measurements of seasonal survival, density, per-capita resource availability and fitness, ideally integrated with historical climatic exposure.

GENERAL CONCLUSIONS

Seasonal resource limitation emerges as a major driver of clutch-size macroevolution across Passeriformes, consistent with a macroevolutionary link between the population-level demographic mechanism proposed by Ashmole and persistent evolutionary differences among species. Among the environmental and life-history factors examined, climate seasonality made the largest contribution to interspecific variation, with annual resource minima contributing far more strongly than resource maxima, highlighting the severity of the resource bottleneck as the principal climatic component identified by our analyses. Climatic seasonality was associated with 33.7% of directional shifts, and the latitudinal gradient was consistent with similar amounts of climate-associated directional change acting in opposite directions: towards reductions in mean clutch size in tropical lineages and increases at higher latitudes, rather than with a greater overall amount of directional evolution at higher latitudes. Seasonality was also associated with 21.5% of evolvability shifts, all of which were accelerations above the background evolutionary rate. Body mass and egg mass were associated with mean clutch size but did not modify the climate-clutch size relationship, suggesting that their associations largely reflect constraints on reproductive allocation rather than differences in climatic sensitivity. Migration, in contrast, revealed that similar contemporary climate-clutch size relationships can conceal distinct evolutionary histories: resident and migratory species responded similarly to climatic

seasonality, yet resident lineages accumulated stronger positive climate-associated directional change, consistent with greater exposure to local seasonal bottlenecks, whereas migration allows species to track seasonal resources while imposing a different set of demographic pressures. Together, these results show that contemporary climatic seasonality is associated with both the direction and tempo of clutch-size evolution, providing a macroevolutionary pattern consistent with Ashmole's population-level mechanism and with the geographical gradient in avian fecundity.

APPENDICES

Supplementary Table S1. Predictors of climate-associated pathwise evolutionary event accumulation.

Pathwise event count	Predictor	β [95% CrI]	Bulk ESS	Tail ESS
Evolvability	Body mass	0.92 [-0.10, 1.99]	1,407	1,225
	Egg mass	0.08 [-1.25, 1.34]	1,338	1,529
	Migration	0.13 [-0.29, 0.58]	1,780	1,430
	Latitudinal zone	-0.13 [-0.51, 0.26]	1,760	1,508
Directional +	Body mass	0.10 [-0.73, 0.97]	1,599	1,427
	Egg mass	0.29 [-0.88, 1.50]	1,479	1,306
	Migration	-0.08 [-0.34, 0.19]	1,671	1,675
	Latitudinal zone	**0.27 [0.02, 0.53]**	2,041	1,779
Directional -	Body mass	0.07 [-1.00, 1.12]	2,171	1,598
	Egg mass	0.74 [-0.63, 2.14]	2,090	1,370
	Migration	-0.21 [-0.66, 0.25]	2,416	1,699
	Latitudinal zone	**-1.22 [-1.72, -0.74]**	3,224	1,804
Directional total	Body mass	-0.00 [-0.71, 0.77]	1,366	1,443
	Egg mass	0.70 [-0.30, 1.66]	1,276	1,652
	Migration	-0.14 [-0.36, 0.08]	1,803	1,644
	Latitudinal zone	-0.14 [-0.36, 0.07]	1,859	1,515

Values are posterior mean coefficients with 95% credible intervals. Bold coefficients indicate 95% credible intervals excluding zero. Models used a Poisson distribution with a log link, an offset for the number of branches along each root-to-tip path, and a phylogenetic random effect. Migration was coded as 0 = resident and 1 = migrant; latitudinal zone as 0 = tropical and 1 = temperate/polar. n = 1663

Supplementary Table S2. Life-history correlates of climate-associated evolutionary event accumulation within major passerine clades.

Pathwise event count	Clade	Body mass	Egg mass	Migration
Evolvability	Tyranni	0.94 [-0.28, 2.19]	0.07 [-1.38, 1.54]	0.27 [-0.57, 1.09]
	Meliphagides	1.53 [-0.47, 3.50]	0.39 [-1.88, 2.70]	0.36 [-1.44, 2.01]
	Corvides	0.92 [-0.74, 2.59]	-0.08 [-2.24, 2.07]	-0.21 [-1.27, 0.74]
	Sylviida	1.80 [-0.08, 3.67]	0.45 [-1.80, 2.71]	0.57 [-0.62, 1.72]
	Muscicapida	0.27 [-1.55, 2.09]	-0.76 [-2.91, 1.45]	0.26 [-0.60, 1.12]
	Passerida	0.82 [-0.70, 2.31]	0.28 [-1.68, 2.22]	0.07 [-0.47, 0.60]
Directional +	Tyranni	-0.20 [-1.26, 0.84]	0.07 [-1.16, 1.28]	-0.68 [-1.47, 0.06]
	Meliphagides	-0.05 [-2.06, 1.92]	0.09 [-2.14, 2.31]	-0.80 [-2.84, 1.14]
	Corvides	0.64 [-0.57, 1.86]	0.59 [-1.22, 2.41]	-0.06 [-0.61, 0.46]
	Sylviida	-1.32 [-3.16, 0.47]	-0.80 [-2.85, 1.27]	**-1.91 [-3.50, -0.61]**
	Muscicapida	-0.00 [-0.89, 0.88]	-0.11 [-1.29, 1.06]	-0.09 [-0.30, 0.13]
	Passerida	0.37 [-1.39, 2.09]	0.26 [-1.71, 2.25]	**-1.41 [-2.86, -0.21]**
Directional -	Tyranni	0.29 [-0.99, 1.55]	0.67 [-0.78, 2.14]	-0.39 [-1.40, 0.62]
	Meliphagides	0.45 [-1.77, 2.63]	0.70 [-1.72, 3.08]	-0.46 [-2.59, 1.64]
	Corvides	-0.33 [-2.47, 1.72]	0.13 [-2.23, 2.44]	-0.64 [-2.69, 1.26]

Pathwise event count	Clade	Body mass	Egg mass	Migration
	Sylviida	1.16 [-0.69, 3.01]	1.35 [-0.83, 3.54]	0.21 [-0.81, 1.17]
	Muscicapida	-0.04 [-1.75, 1.70]	0.42 [-1.71, 2.52]	-0.87 [-2.02, 0.17]
	Passerida	-0.25 [-1.66, 1.14]	0.93 [-0.92, 2.76]	-0.17 [-0.74, 0.38]
Directional total	Tyranni	-0.14 [-1.11, 0.85]	0.75 [-0.42, 1.92]	-0.31 [-1.07, 0.41]
	Meliphagides	0.07 [-1.89, 2.04]	0.77 [-1.46, 2.91]	-0.48 [-2.50, 1.35]
	Corvides	0.29 [-1.01, 1.60]	1.08 [-0.75, 2.90]	-0.01 [-0.60, 0.56]
	Sylviida	0.22 [-1.32, 1.74]	1.02 [-0.91, 2.90]	-0.68 [-1.50, 0.06]
	Muscicapida	-0.13 [-1.15, 0.86]	0.17 [-1.15, 1.53]	0.05 [-0.20, 0.31]
	Passerida	-0.77 [-1.93, 0.39]	**1.63 [0.09, 3.14]**	**-0.87 [-1.31, -0.44]**

Values are posterior median coefficients with 95% credible intervals from phylogenetic Poisson models. Coefficients represent within-clade associations between each life-history trait and the number of climate-associated evolutionary events accumulated along root-to-tip paths. Bold coefficients indicate 95% credible intervals excluding zero. Models included an offset for the number of branches along each root-to-tip path and a phylogenetic random effect. Migration was coded as 0 = resident and 1 = migrant. n = 1624

Supplementary Table S3. Predictors of climate-associated pathwise evolutionary event magnitude.

Pathwise event magnitude	Predictor	Median β	95% HPD	ESS
Evolvability	Body mass	0.1380	[-0.0449, 0.2798]	1,351
	Egg mass	-0.0545	[-0.3045, 0.1557]	1,371
	Migration	-0.0016	[-0.0354, 0.0320]	1,001
	Latitudinal zone	-0.0155	[-0.0456, 0.0155]	1,001
Directional +	Body mass	-0.0064	[-0.0142, 0.0011]	686
	Egg mass	0.0063	[-0.0038, 0.0175]	827
	Migration	**-0.0019**	**[-0.0036, -0.0005]**	686
	Latitudinal zone	**0.0040**	**[0.0028, 0.0055]**	686
Directional -	Body mass	0.0056	[-0.0024, 0.0131]	1,001
	Egg mass	0.0011	[-0.0098, 0.0126]	1,001
	Migration	0.0004	[-0.0013, 0.0021]	1,001
	Latitudinal zone	**-0.0031**	**[-0.0047, -0.0016]**	1,001
Directional total	Body mass	-0.0012	[-0.0117, 0.0088]	1,001
	Egg mass	0.0081	[-0.0074, 0.0223]	1,001
	Migration	-0.0015	[-0.0036, 0.0006]	1,001
	Latitudinal zone	0.0012	[-0.0007, 0.0032]	1,001

Values are posterior median regression coefficients with 95% highest posterior density (HPD) intervals. Bold coefficients indicate 95% HPD intervals excluding zero. ESS denotes effective sample size. Pathwise evolutionary metrics were log10(x + 1)-transformed.

Supplementary Table S4. Stepwise regression models under the Fabric model

Parameter	M1	M2	M3	M4	M5	M6	M7	M8	M9	M10
Body mass	**0.141 [0.076, 0.203]**	**0.130 [0.077, 0.186]**	**0.132 [0.076, 0.184]**	**0.136 [0.079, 0.190]**	**0.135 [0.080, 0.189]**	**0.136 [0.083, 0.188]**	**0.136 [0.083, 0.192]**	**0.137 [0.083, 0.189]**	**0.136 [0.080, 0.189]**	**0.136 [0.080, 0.189]**
Egg mass	**-0.209 [-0.296, -0.118]**	**-0.197 [-0.274, -0.121]**	**-0.195 [-0.272, -0.113]**	**-0.201 [-0.276, -0.121]**	**-0.198 [-0.277, -0.124]**	**-0.194 [-0.270, -0.118]**	**-0.196 [-0.273, -0.123]**	**-0.196 [-0.274, -0.122]**	**-0.196 [-0.270, -0.114]**	**-0.195 [-0.271, -0.119]**
Emax	0.007 [-0.052, 0.065]	0.011 [-0.044, 0.065]	0.009 [-0.047, 0.071]	0.009 [-0.050, 0.066]	-0.007 [-0.049, 0.034]	-0.009 [-0.054, 0.035]	-0.010 [-0.052, 0.033]	-0.017 [-0.058, 0.021]	-0.019 [-0.057, 0.018]	-0.019 [-0.058, 0.022]
Emin	**-0.114 [-0.140, -0.090]**	**-0.118 [-0.142, -0.094]**	**-0.118 [-0.143, -0.093]**	**-0.116 [-0.140, -0.093]**	**-0.110 [-0.127, -0.090]**	**-0.109 [-0.128, -0.090]**	**-0.108 [-0.126, -0.090]**	**-0.101 [-0.113, -0.088]**	**-0.100 [-0.111, -0.088]**	**-0.100 [-0.112, -0.088]**
Migration	**0.058 [0.046, 0.070]**	**0.059 [0.047, 0.070]**	**0.058 [0.047, 0.070]**	**0.058 [0.047, 0.070]**	**0.060 [0.049, 0.071]**	**0.061 [0.050, 0.072]**	**0.061 [0.051, 0.072]**	**0.062 [0.051, 0.072]**	**0.063 [0.052, 0.073]**	**0.062 [0.051, 0.073]**
Body mass × egg mass	0.013 [-0.042, 0.065]	0.012 [-0.044, 0.067]								
Body mass × Emax	-0.113 [-0.376, 0.135]	-0.134 [-0.391, 0.103]	-0.128 [-0.387, 0.121]	-0.052 [-0.146, 0.037]	-0.052 [-0.144, 0.043]	-0.045 [-0.139, 0.051]				
Body mass × Emin	0.104 [-0.013, 0.232]	**0.118 [0.009, 0.224]**	**0.118 [0.010, 0.234]**	**0.095 [0.005, 0.184]**	0.086 [-0.005, 0.175]	0.083 [-0.006, 0.173]	0.069 [-0.014, 0.154]	0.064 [-0.022, 0.152]	0.018 [-0.009, 0.045]	
Body mass × migration	-0.034 [-0.142, 0.077]									
Egg mass × Emax	0.100 [-0.260, 0.469]	0.129 [-0.216, 0.496]	0.121 [-0.229, 0.492]							
Egg mass × Emin	-0.105 [-0.274, 0.060]	-0.121 [-0.269, 0.032]	-0.123 [-0.291, 0.029]	-0.085 [-0.204, 0.033]	-0.074 [-0.195, 0.045]	-0.078 [-0.195, 0.040]	-0.068 [-0.185, 0.042]	-0.067 [-0.189, 0.056]		
Egg mass × migration	0.064 [-0.087, 0.212]	0.020 [-0.017, 0.059]	0.020 [-0.019, 0.058]	0.019 [-0.018, 0.059]	0.019 [-0.020, 0.057]					
Emax × Emin	**-0.117 [-0.163, -0.073]**	**-0.116 [-0.161, -0.073]**	**-0.118 [-0.165, -0.073]**	**-0.117 [-0.163, -0.075]**	**-0.117 [-0.160, -0.074]**	**-0.117 [-0.162, -0.075]**	**-0.114 [-0.158, -0.073]**	**-0.113 [-0.159, -0.073]**	**-0.117 [-0.158, -0.075]**	**-0.115 [-0.161, -0.074]**
Emax × migration	-0.024 [-0.089, 0.042]	-0.026 [-0.089, 0.036]	-0.028 [-0.094, 0.039]	-0.030 [-0.095, 0.035]						
Emin × migration	0.016 [-0.012, 0.045]	0.019 [-0.006, 0.046]	0.020 [-0.009, 0.047]	0.019 [-0.006, 0.047]	0.011 [-0.009, 0.030]	0.012 [-0.009, 0.032]	0.010 [-0.009, 0.030]			

Values are posterior medians [90% equal-tailed credible intervals]. Bold indicates that at least 95% of the posterior distribution lies either above or below zero. Emax and Emin denote the maximum and minimum annual values of actual terrestrial evaporation, respectively.

Supplementary Table S5. Stepwise regression models under the variable-rates model

Parameter	M1	M2	M3	M4	M5	M6	M7	M8	M9	M10
Body mass	**0.150 [0.081, 0.211]**	**0.133 [0.079, 0.188]**	**0.135 [0.083, 0.192]**	**0.134 [0.080, 0.191]**	**0.137 [0.084, 0.191]**	**0.138 [0.082, 0.190]**	**0.138 [0.082, 0.192]**	**0.136 [0.086, 0.189]**	**0.139 [0.086, 0.195]**	**0.140 [0.088, 0.190]**
Egg mass	**-0.222 [-0.306, -0.129]**	**-0.201 [-0.275, -0.124]**	**-0.198 [-0.277, -0.123]**	**-0.197 [-0.276, -0.118]**	**-0.202 [-0.278, -0.127]**	**-0.197 [-0.270, -0.117]**	**-0.198 [-0.275, -0.119]**	**-0.195 [-0.266, -0.123]**	**-0.199 [-0.277, -0.119]**	**-0.198 [-0.271, -0.126]**
Emax	0.005 [-0.052, 0.065]	0.007 [-0.051, 0.061]	0.007 [-0.049, 0.063]	0.007 [-0.050, 0.065]	-0.014 [-0.058, 0.031]	-0.014 [-0.056, 0.028]	-0.016 [-0.058, 0.028]	-0.020 [-0.061, 0.020]	-0.023 [-0.062, 0.017]	-0.022 [-0.060, 0.017]
Emin	**-0.114 [-0.139, -0.088]**	**-0.115 [-0.139, -0.092]**	**-0.116 [-0.139, -0.091]**	**-0.115 [-0.140, -0.091]**	**-0.107 [-0.126, -0.089]**	**-0.107 [-0.127, -0.088]**	**-0.106 [-0.126, -0.088]**	**-0.100 [-0.113, -0.088]**	**-0.099 [-0.111, -0.087]**	**-0.100 [-0.112, -0.088]**
Migration	**0.055 [0.043, 0.066]**	**0.056 [0.044, 0.067]**	**0.056 [0.044, 0.067]**	**0.056 [0.044, 0.067]**	**0.057 [0.046, 0.068]**	**0.058 [0.047, 0.069]**	**0.058 [0.047, 0.069]**	**0.059 [0.048, 0.069]**	**0.059 [0.049, 0.070]**	**0.059 [0.048, 0.069]**
Body mass × egg mass	0.015 [-0.036, 0.067]	0.016 [-0.039, 0.070]								
Body mass × Emax	-0.070 [-0.342, 0.196]	-0.088 [-0.348, 0.166]	-0.092 [-0.339, 0.166]	-0.048 [-0.148, 0.046]	-0.047 [-0.140, 0.047]	-0.043 [-0.137, 0.053]				
Body mass × Emin	0.095 [-0.025, 0.220]	**0.115 [0.001, 0.237]**	**0.119 [0.009, 0.231]**	**0.107 [0.015, 0.201]**	**0.097 [0.010, 0.187]**	**0.092 [0.002, 0.183]**	0.080 [-0.005, 0.163]	0.074 [-0.008, 0.159]	0.023 [-0.004, 0.051]	
Body mass × migration	-0.054 [-0.161, 0.051]									
Egg mass × Emax	0.034 [-0.329, 0.428]	0.066 [-0.293, 0.426]	0.067 [-0.302, 0.417]							
Egg mass × Emin	-0.084 [-0.259, 0.076]	-0.112 [-0.278, 0.039]	-0.116 [-0.267, 0.034]	-0.097 [-0.218, 0.021]	-0.085 [-0.205, 0.027]	-0.086 [-0.202, 0.033]	-0.082 [-0.196, 0.040]	-0.074 [-0.193, 0.036]		
Egg mass × migration	0.090 [-0.060, 0.229]	0.020 [-0.019, 0.058]	0.019 [-0.021, 0.058]	0.017 [-0.023, 0.058]	0.018 [-0.020, 0.056]					
Emax × Emin	**-0.122 [-0.170, -0.076]**	**-0.121 [-0.173, -0.079]**	**-0.122 [-0.167, -0.079]**	**-0.122 [-0.171, -0.077]**	**-0.123 [-0.168, -0.079]**	**-0.123 [-0.165, -0.082]**	**-0.121 [-0.164, -0.078]**	**-0.120 [-0.164, -0.079]**	**-0.123 [-0.168, -0.080]**	**-0.124 [-0.165, -0.082]**
Emax × migration	-0.035 [-0.100, 0.029]	-0.033 [-0.098, 0.034]	-0.033 [-0.100, 0.032]	-0.038 [-0.102, 0.030]						
Emin × migration	0.015 [-0.015, 0.044]	0.018 [-0.009, 0.044]	0.018 [-0.009, 0.046]	0.019 [-0.007, 0.047]	0.009 [-0.012, 0.029]	0.009 [-0.010, 0.029]	0.008 [-0.012, 0.028]			

Values are posterior medians [90% equal-tailed credible intervals]. Bold indicates that at least 95% of the posterior distribution lies either above or below zero. Emax and Emin denote the maximum and minimum annual values of actual terrestrial evaporation, respectively.

Supplementary Table S6. Stepwise regression models under the Brownian-motion model

Parameter	M1	M2	M3	M4	M5	M6	M7
Body mass	**0.109 [0.046, 0.169]**	**0.108 [0.042, 0.165]**	**0.107 [0.045, 0.168]**	**0.105 [0.043, 0.172]**	**0.108 [0.045, 0.171]**	**0.094 [0.035, 0.149]**	**0.095 [0.039, 0.150]**
Egg mass	**-0.164 [-0.248, -0.075]**	**-0.165 [-0.247, -0.076]**	**-0.165 [-0.247, -0.078]**	**-0.162 [-0.252, -0.072]**	**-0.164 [-0.250, -0.078]**	**-0.146 [-0.220, -0.062]**	**-0.149 [-0.225, -0.072]**
Emax	-0.024 [-0.081, 0.032]	-0.025 [-0.083, 0.034]	-0.026 [-0.083, 0.031]	-0.023 [-0.079, 0.033]	-0.039 [-0.086, 0.007]	-0.042 [-0.086, 0.004]	**-0.052 [-0.094, -0.011]**
Emin	**-0.105 [-0.130, -0.083]**	**-0.105 [-0.131, -0.082]**	**-0.105 [-0.130, -0.081]**	**-0.106 [-0.129, -0.082]**	**-0.097 [-0.110, -0.082]**	**-0.096 [-0.109, -0.082]**	**-0.095 [-0.108, -0.082]**
Migration	**0.045 [0.033, 0.056]**	**0.044 [0.033, 0.056]**	**0.045 [0.034, 0.057]**	**0.045 [0.033, 0.056]**	**0.046 [0.034, 0.057]**	**0.047 [0.035, 0.058]**	**0.046 [0.036, 0.058]**
Body mass × egg mass	-0.014 [-0.068, 0.044]						
Body mass × Emax	-0.050 [-0.330, 0.235]	-0.057 [-0.328, 0.226]					
Body mass × Emin	**0.135 [0.018, 0.255]**	**0.139 [0.018, 0.257]**	**0.124 [0.032, 0.214]**	**0.121 [0.029, 0.216]**	**0.113 [0.019, 0.208]**	**0.126 [0.037, 0.220]**	**0.126 [0.036, 0.214]**
Body mass × migration	-0.078 [-0.181, 0.030]	-0.077 [-0.179, 0.026]	-0.076 [-0.176, 0.030]	-0.079 [-0.183, 0.029]	-0.088 [-0.197, 0.014]	**-0.039 [-0.069, -0.011]**	**-0.038 [-0.066, -0.009]**
Egg mass × Emax	0.106 [-0.288, 0.493]	0.105 [-0.289, 0.484]	0.037 [-0.106, 0.168]				
Egg mass × Emin	**-0.184 [-0.343, -0.027]**	**-0.185 [-0.348, -0.025]**	**-0.168 [-0.299, -0.041]**	**-0.162 [-0.285, -0.027]**	**-0.145 [-0.278, -0.018]**	**-0.166 [-0.290, -0.048]**	**-0.165 [-0.287, -0.045]**
Egg mass × migration	0.055 [-0.094, 0.198]	0.055 [-0.089, 0.194]	0.050 [-0.095, 0.193]	0.054 [-0.094, 0.194]	0.069 [-0.071, 0.211]		
Emax × Emin	**-0.192 [-0.235, -0.143]**	**-0.191 [-0.235, -0.144]**	**-0.191 [-0.235, -0.147]**	**-0.191 [-0.236, -0.144]**	**-0.193 [-0.239, -0.146]**	**-0.194 [-0.237, -0.148]**	**-0.191 [-0.236, -0.145]**
Emax × migration	-0.054 [-0.126, 0.015]	-0.056 [-0.126, 0.017]	-0.055 [-0.126, 0.011]	-0.058 [-0.127, 0.007]	-0.039 [-0.094, 0.019]	-0.033 [-0.087, 0.023]	
Emin × migration	0.013 [-0.015, 0.041]	0.013 [-0.015, 0.043]	0.012 [-0.015, 0.041]	0.015 [-0.015, 0.041]			

Values are posterior medians [90% equal-tailed credible intervals]. Bold indicates that at least 95% of the posterior distribution lies either above or below zero. Emax and Emin denote the maximum and minimum annual values of actual terrestrial evaporation, respectively.

Supplementary Table S7. Comparison of the final evolutionary models using marginal likelihoods

Comparison	Mean marginal likelihood complex model	Mean marginal likelihood simple model	Bayes Factor	Preferred model	Evidence
Fabric (M10) vs. Variable rates (M10)	1569.02	1465.06	207.93	Fabric (M10)	Very strong
Fabric (M10) vs. Brownian motion (M7)	1569.02	1185.22	767.61	Fabric (M10)	Very strong
Variable rates (M10) vs. Brownian motion (M7)	1465.06	1185.22	559.68	Variable rates (M10)	Very strong

Marginal likelihoods are means across stepping-stone replicates. Bayes Factor= 2 × (Marginal likelihood Complex model − Marginal likelihood Simple model); positive values favour complex models, and negative values favour simpler models. Evidence categories are based on the absolute magnitude of Bayes Factor: 0–2 weak, 2–5 positive, 5–10 strong, and >10 very strong.

BIBLIOGRAPHIC REFERENCES

Ashmole, N. P. (1961). *The biology of certain terns, with special reference to the black noddy, Anoüs tenuirostris, and the wideawake, Sterna fuscata on Ascension Island* [Electronic Thesis or Dissertation, University of Oxford]. British Library EThOS. https://search.ebscohost.com/login.aspx?direct=true&AuthType=sso&db=edsble&AN=edsble.671562&lang=es&site=eds-live&scope=site&custid=s7489523

Ashmole, N. P. (1963). THE REGULATION OF NUMBERS OF TROPICAL OCEANIC BIRDS [https://doi.org/10.1111/j.1474-919X.1963.tb06766.x]. *Ibis*, *103b*(3), 458-473. https://doi.org/10.1111/j.1474-919X.1963.tb06766.x

Baker, J., Meade, A., Pagel, M., & Venditti, C. (2015a). Adaptive evolution toward larger size in mammals. *Proceedings of the National Academy of Sciences of the United States of America*, *112*, 5093–5098. https://doi.org/10.1073/pnas.1419823112

Baker, J., Meade, A., Pagel, M., & Venditti, C. (2015b). Positive phenotypic selection inferred from phylogenies. *Biological Journal of the Linnean Society*, *118*, n/a-n/a. https://doi.org/10.1111/bij.12649

Baker, J., & Venditti, C. (2019). Rapid Change in Mammalian Eye Shape Is Explained by Activity Pattern. *Current Biology*, *29*(6), 1082-1088.e1083. https://doi.org/10.1016/j.cub.2019.02.017

Bell, F., Ouwehand, J., Both, C., Briedis, M., Lisovski, S., Wang, X., Bearhop, S., & Burgess, M. (2024). Individuals departing non-breeding areas early achieve earlier breeding and higher breeding success. *Scientific Reports*, *14*(1), 4075. https://doi.org/10.1038/s41598-024-53575-2

Boyer, A. G., Cartron, J.-L. E., & Brown, J. H. (2010). Interspecific pairwise relationships among body size, clutch size and latitude: deconstructing a macroecological triangle in birds. *Journal of Biogeography*, *37*(1), 47-56. https://doi.org/10.1111/j.1365-2699.2009.02175.x

Brown, J. H., Gillooly, J. F., Allen, A. P., Savage, V. M., & West, G. B. (2004). TOWARD A METABOLIC THEORY OF ECOLOGY. *Ecology*, *85*(7), 1771-1789. https://doi.org/10.1890/03-9000

Brown, J. H., Hall, C. A. S., & Sibly, R. M. (2018). Equal fitness paradigm explained by a trade-off between generation time and energy production rate. *Nature Ecology & Evolution*, *2*(2), 262-268. https://doi.org/10.1038/s41559-017-0430-1

Brown, J. H., & Sibly, R. M. (2006). Life-history evolution under a production constraint. *Proceedings of the National Academy of Sciences*, *103*(47), 17595-17599. https://doi.org/10.1073/pnas.0608522103

Burger, J. R., Hou, C., & Brown, J. H. (2019). Toward a metabolic theory of life history. *Proceedings of the National Academy of Sciences*, *116*(52), 26653-26661. https://doi.org/10.1073/pnas.1907702116

Bürkner, P.-C. (2017). brms: An R Package for Bayesian Multilevel Models Using Stan. *Journal of Statistical Software*, *80*(1), 1 - 28. https://doi.org/10.18637/jss.v080.i01

Calder, W. A. (1984). *Size, function and life history*. Harvard University Press.

Chik, H. Y. J., Estrada, C., Wang, Y., Tank, P., Lord, A., & Schroeder, J. (2022). Individual variation in reaction norms but no directional selection in reproductive plasticity of a wild passerine population. *Ecology and Evolution*, *12*(2), e8582. https://doi.org/10.1002/ece3.8582

Drury, J. P., Clavel, J., Tobias, J. A., Rolland, J., Sheard, C., & Morlon, H. (2021). Tempo and mode of morphological evolution are decoupled from latitude in birds. *PLoS biology*, *19*(8), e3001270. https://doi.org/10.1371/journal.pbio.3001270

Ducatez, S., & Field, D. J. (2021). Disentangling the avian altricial-precocial spectrum: Quantitative assessment of developmental mode, phylogenetic signal, and dimensionality. *Evolution*, *75*(11), 2717-2735. https://doi.org/10.1111/evo.14365

Evans, S. R., Postma, E., & Sheldon, B. C. (2020). It takes two: Heritable male effects on reproductive timing but not clutch size in a wild bird population. *Evolution*, *74*(10), 2320-2331. https://doi.org/10.1111/evo.13980

Eyres, A., Böhning-Gaese, K., Orme, C. D. L., Rahbek, C., & Fritz, S. A. (2020). A tale of two seasons: The link between seasonal migration and climatic niches in passerine birds. *Ecology and Evolution*, *10*(21), 11983-11997. https://doi.org/10.1002/ece3.6729

Felsenstein, J. (1985). Phylogenies and the Comparative Method. *The American Naturalist*, *125*(1), 1-15. http://www.jstor.org/stable/2461605

Furness, A. I., Venditti, C., & Capellini, I. (2022). Terrestrial reproduction and parental care drive rapid evolution in the trade-off between offspring size and number across amphibians. *PLoS biology*, *20*(1), e3001495. https://doi.org/10.1371/journal.pbio.3001495

Gould, S. J. (1988). Trends as Changes in Variance: A New Slant on Progress and Directionality in Evolution. *Journal of Paleontology*, *62*(3), 319-329. http://www.jstor.org/stable/1305411

Griebeler, E. M., & Böhning-Gaese, K. (2004). Evolution of clutch size along latitudinal gradients: revisiting Ashmole's hypothesis. *Evolutionary Ecology Research*, *6*, 679-694.

Griebeler, E. M., Caprano, T., & Böhning-Gaese, K. (2010). Evolution of avian clutch size along latitudinal gradients: do seasonality, nest predation or breeding season length matter? *Journal of Evolutionary Biology*, *23*(5), 888-901. https://doi.org/10.1111/j.1420-9101.2010.01958.x

Haywood, S. (2013). Origin of evolutionary change in avian clutch size. *Biological Reviews*, *88*(4), 895-911. https://doi.org/10.1111/brv.12035

Hidalgo Aranzamendi, N., Hall, M. L., Kingma, S. A., van de Pol, M., & Peters, A. (2019). Rapid plastic breeding response to rain matches peak prey abundance in a tropical savanna bird. *Journal of Animal Ecology*, *88*(11), 1799-1811. https://doi.org/10.1111/1365-2656.13068

Hořák, D., Tószögyová, A., & Storch, D. (2015). Relative food limitation drives geographical clutch size variation in South African passerines: a large-scale test of Ashmole's seasonality hypothesis. *Global Ecology and Biogeography*, *24*(4), 437-447. https://doi.org/10.1111/geb.12261

Husby, A., Kawakami, T., Rönnegård, L., Smeds, L., Ellegren, H., & Qvarnström, A. (2015). Genome-wide association mapping in a wild avian population identifies a link

between genetic and phenotypic variation in a life-history trait. *Proceedings of the Royal Society B: Biological Sciences*, *282*.
Jetz, W., Sekercioglu, C. H., & Böhning-Gaese, K. (2008). The worldwide variation in avian clutch size across species and space. *PLoS biology*, *6*(12), 2650-2657. https://doi.org/10.1371/journal.pbio.0060303
Lack, D. (1947). The Significance of Clutch-size [https://doi.org/10.1111/j.1474-919X.1947.tb04155.x]. *Ibis*, *89*(2), 302-352. https://doi.org/10.1111/j.1474-919X.1947.tb04155.x
Lack, D. L. (1967). The significance of clutch-size in waterfowl.
Lechki, S. C., & Benson, R. B. J. (2026). Evolutionary drivers of reproductive output variation among amniotes, and the origins of large offspring in birds. *Royal Society Open Science*, *13*(6), 251708. https://doi.org/10.1098/rsos.251708
Lindner, M., Verhagen, I., Mateman, A. C., van Oers, K., Laine, V. N., & Visser, M. E. (2024). Genetic and epigenetic differentiation in response to genomic selection for avian lay date. *Evolutionary Applications*, *17*(7), e13703. https://doi.org/10.1111/eva.13703
Liu, M., Rubenstein, D. R., Cheong, S.-A., & Shen, S.-F. (2018). Multitasking and the evolution of optimal clutch size in fluctuating environments [https://doi.org/10.1002/ece3.4364]. *Ecology and Evolution*, *8*(17), 8803-8817. https://doi.org/10.1002/ece3.4364
Lundblad, C. G., & Conway, C. J. (2021). Ashmole's hypothesis and the latitudinal gradient in clutch size [https://doi.org/10.1111/brv.12705]. *Biological Reviews*, *96*(4), 1349-1366. https://doi.org/10.1111/brv.12705
Lundblad, C. G., & Conway, C. J. (2023). Investing in a nest egg: intraspecific variation in the timing of egg laying across a latitudinal gradient. *Oecologia*, *202*(1), 83-96. https://doi.org/10.1007/s00442-023-05373-2
Martin, E. C., Hansen, B. B., Lee, A. M., & Herfindal, I. (2023). Generation time and seasonal migration explain variation in spatial population synchrony across European bird species. *Journal of Animal Ecology*, *92*(9), 1904-1918. https://doi.org/10.1111/1365-2656.13983
Martin, J. S., Westneat, D. F., Nakagawa, S., Schroeder, J., & Burke, T. (2025). Measuring selection on reaction norms: Lack's principle and plasticity in clutch size. *Evolution*, *79*(11), 2460-2473. https://doi.org/10.1093/evolut/qpaf168
Martin, T. E., Bassar, R. D., Bassar, S. K., Fontaine, J. J., Lloyd, P., Mathewson, H. A., Niklison, A. M., & Chalfoun, A. (2006). LIFE-HISTORY AND ECOLOGICAL CORRELATES OF GEOGRAPHIC VARIATION IN EGG AND CLUTCH MASS AMONG PASSERINE SPECIES. *Evolution*, *60*(2), 390-398. https://doi.org/10.1111/j.0014-3820.2006.tb01115.x
Martin, T. E. (2015). Age-related mortality explains life history strategies of tropical and temperate songbirds. *Science*, *349*(6251), 966-970. https://doi.org/10.1126/science.aad1173
McTavish, E. J., Gerbracht, J. A., Holder, M. T., Iliff, M. J., Lepage, D., Rasmussen, P. C., Redelings, B. D., Sánchez Reyes, L. L., & Miller, E. T. (2025). A complete and dynamic tree of birds. *Proceedings of the National Academy of Sciences*, *122*(18), e2409658122. https://doi.org/10.1073/pnas.2409658122

Meiri, S., Avila, L., Bauer, A. M., Chapple, D. G., Das, I., Doan, T. M., Doughty, P., Ellis, R., Grismer, L., Kraus, F., Morando, M., Oliver, P., Pincheira-Donoso, D., Ribeiro-Junior, M. A., Shea, G., Torres-Carvajal, O., Slavenko, A., & Roll, U. (2020). The global diversity and distribution of lizard clutch sizes [https://doi.org/10.1111/geb.13124]. *Global Ecology and Biogeography*, *29*(9), 1515-1530. https://doi.org/10.1111/geb.13124

Miralles, D. G., Bonte, O., Koppa, A., Baez-Villanueva, O. M., Tronquo, E., Zhong, F., Beck, H. E., Hulsman, P., Dorigo, W., Verhoest, N. E. C., & Haghdoost, S. (2025). GLEAM4: global land evaporation and soil moisture dataset at 0.1° resolution from 1980 to near present. *Scientific Data*, *12*(1), 416. https://doi.org/10.1038/s41597-025-04610-y

Moreau, R. E. (1944). Clutch-size: A Comparative Study, with Special Reference to African Birds [https://doi.org/10.1111/j.1474-919X.1944.tb04093.x]. *Ibis*, *86*(3), 286-347. https://doi.org/10.1111/j.1474-919X.1944.tb04093.x

O'Meara, B. C., Ané, C., Sanderson, M. J., & Wainwright, P. C. (2006). TESTING FOR DIFFERENT RATES OF CONTINUOUS TRAIT EVOLUTION USING LIKELIHOOD. *Evolution*, *60*(5), 922-933. https://doi.org/10.1111/j.0014-3820.2006.tb01171.x

Okie, J. G., Boyer, A. G., Brown, J. H., Costa, D. P., Ernest, S. K. M., Evans, A. R., Fortelius, M., Gittleman, J. L., Hamilton, M. J., Harding, L. E., Lintulaakso, K., Lyons, S. K., Saarinen, J. J., Smith, F. A., Stephens, P. R., Theodor, J., Uhen, M. D., & Sibly, R. M. (2013). Effects of allometry, productivity and lifestyle on rates and limits of body size evolution. *Proceedings of the Royal Society B: Biological Sciences*, *280*(1764), 20131007. https://doi.org/10.1098/rspb.2013.1007

Pagel, M., & Meade, A. (2025). Trait macroevolution in the presence of covariates. *Nature Communications*, *16*. https://doi.org/10.1038/s41467-025-59836-6

Pagel, M., O'Donovan, C., & Meade, A. (2022). General statistical model shows that macroevolutionary patterns and processes are consistent with Darwinian gradualism. *Nature Communications*, *13*(1), 1113. https://doi.org/10.1038/s41467-022-28595-z

Pienaar, J., Ilany, A., Geffen, E., & Yom-Tov, Y. (2013). Macroevolution of life-history traits in passerine birds: adaptation and phylogenetic inertia [https://doi.org/10.1111/ele.12077]. *Ecology Letters*, *16*(5), 571-576. https://doi.org/10.1111/ele.12077

Pincheira-Donoso, D., & Hunt, J. (2017). Fecundity selection theory: concepts and evidence [https://doi.org/10.1111/brv.12232]. *Biological Reviews*, *92*(1), 341-356. https://doi.org/10.1111/brv.12232

Postma, E., & van Noordwijk, A. J. (2005). Gene flow maintains a large genetic difference in clutch size at a small spatial scale. *Nature*, *433*(7021), 65-68. https://doi.org/10.1038/nature03083

Ramakers, J. J. C., Cobben, M. M. P., Bijma, P., Reed, T. E., Visser, M. E., & Gienapp, P. (2018). Maternal Effects in a Wild Songbird Are Environmentally Plastic but Only Marginally Alter the Rate of Adaptation. *The American Naturalist*, *191*(5), E144-E158. https://doi.org/10.1086/696847

Revell, L. J., Harmon, L. J., & Collar, D. C. (2008). Phylogenetic Signal, Evolutionary Process, and Rate. *Systematic Biology, 57(4)*, 591-601. https://doi.org/10.1080/10635150802302427

Ricklefs, R. E. (2000). Density Dependence, Evolutionary Optimization, and the Diversification of Avian Life Histories. *The Condor*, *102*(1), 9-22. https://doi.org/10.1093/condor/102.1.9

Rotenberry, J. T., & Balasubramaniam, P. (2020). Estimating egg mass–body mass relationships in birds. *The Auk*, *137*(3). https://doi.org/10.1093/auk/ukaa019

Rowe, L., Ludwig, D., & Schluter, D. (1994). Time, Condition, and the Seasonal Decline of Avian Clutch Size. *The American Naturalist*, *143*(4), 698-722. https://doi.org/10.1086/285627

Scholer, M. N., Strimas-Mackey, M., & Jankowski, J. E. (2020). A meta-analysis of global avian survival across species and latitude. *Ecology Letters*, *23*(10), 1537-1549. https://doi.org/10.1111/ele.13573

Şekercioğlu, Ç. H., Kittelberger, K. D., Mota, F. M. M., Buxton, A. N., Orton, N., DeNiro, A., Buechley, E. R., Horns, J. J., Blount, J. D., Socci, J., & Neate-Clegg, M. H. C. (2025). BIRDBASE: A Global Dataset of Avian Biogeography, Conservation, Ecology and Life History Traits. *Scientific Data*, *12*(1), 1558. https://doi.org/10.1038/s41597-025-05615-3

Sibly, R. M., Kodric-Brown, A., & Brown, J. H. (2012). *Metabolic ecology : a scaling approach* (First published 2012. ed.) [Regular print reproduction

Non-fiction]. Wiley-Blackwell. https://search.ebscohost.com/login.aspx?direct=true&AuthType=sso&db=cat09074a&AN=cbu.oai.folio.org.fs00001060.48b59922.bea1.4043.b8f0.7ef3aee6fa2b&lang=es&site=eds-live&scope=site&custid=s7489523

Sibly, R. M., Witt, C. C., Wright, N. A., Venditti, C., Jetz, W., & Brown, J. H. (2012). Energetics, lifestyle, and reproduction in birds. *Proceedings of the National Academy of Sciences*, *109*(27), 10937-10941. https://doi.org/10.1073/pnas.1206512109

Smith, C. C., & Fretwell, S. D. (1974). The Optimal Balance between Size and Number of Offspring. *The American Naturalist*, *108*(962), 499-506. http://www.jstor.org/stable/2459681

Song, Z., Lin, X., Que, P., Halimubieke, N., Huang, Q., Zhang, Z., Székely, T., & Liu, Y. (2020). The allocation between egg size and clutch size depends on local nest survival rate in a mean of bet-hedging in a shorebird. *Avian Research*, *11*(1), 40. https://doi.org/10.1186/s40657-020-00225-6

Soriano-Redondo, A., Gutiérrez, J. S., Hodgson, D., & Bearhop, S. (2020). Migrant birds and mammals live faster than residents. *Nature Communications*, *11*(1), 5719. https://doi.org/10.1038/s41467-020-19256-0

Stearns, S. C. (1992). *The Evolution of Life Histories*. OUP Oxford. https://books.google.cl/books?id=-NcNAZ06nNoC

Tökölyi, J., Schmidt, J., & Barta, Z. (2014). Climate and mammalian life histories [https://doi.org/10.1111/bij.12238]. *Biological Journal of the Linnean Society*, *111*(4), 719-736. https://doi.org/10.1111/bij.12238

Uyeda, J. C., Hansen, T. F., Arnold, S. J., & Pienaar, J. (2011). The million-year wait for macroevolutionary bursts. *Proceedings of the National Academy of Sciences*, *108*(38), 15908-15913. https://doi.org/10.1073/pnas.1014503108

Varpe, Ø. (2017). Life History Adaptations to Seasonality. *Integrative and Comparative Biology*, *57*(5), 943-960. https://doi.org/10.1093/icb/icx123

Venditti, C., Meade, A., & Pagel, M. (2011). Multiple routes to mammalian diversity. *Nature*, *479*(7373), 393-396. https://doi.org/10.1038/nature10516

Winger, B. M., & Pegan, T. M. (2021). Migration distance is a fundamental axis of the slow-fast continuum of life history in boreal birds. *Ornithology*, *138*(4), ukab043. https://doi.org/10.1093/ornithology/ukab043

Youngflesh, C., Kapsar, K., Uscanga, A., Williams, P. J., Doser, J. W., Kounta, L., & Zarnetske, P. L. (2025). Environmental Variability Shapes Life History of the World's Birds. *Ecology Letters*, *28*(2), e70077. https://doi.org/10.1111/ele.70077